in all the cells of NHD patients, and Syk is not tyrosine-phosphorylated in normal resting cells.[9] However, the possibility exists that Syk expressed in neurons undergoes tyrosine phosphorylation, mediated by non-DAP12 ITAM-containing molecules, such as tamalin, FcRγ and C-type lectin receptors (CLRs) containing ITAM-like motifs, including CLEC2, CLEC7A (Dectin-1) and CLEC9A.[10,28,29] An alternative possibility is that Syk expressed in neurons is activated by various ITAM-independent signals.[9,10] Syk is activated upon stimulation of G-protein-coupled receptors by corresponding ligands.[30] Syk is directly activated by oxidative stress, following treatment of the cells with hydrogen peroxide.[31] The αIIbβ3 integrin activates Syk via direct interaction between the cytoplasmic tail of the integrin β-chain and the non-ITAM-binding SH2 domain of Syk.[32] Even overexpression of Syk induces its autophosphorylation.[9] Our observations that substantial populations of DAP12-deficient microglia expressed pSyk in NHD brains support the possible involvement of either non-DAP12 ITAM-containing molecules or ITAM-independent signals in neuronal activation of Syk in NHD brains. The majority of NHD patients suffer from intractable epileptic seizures in advanced stages of the disease.[3] Therefore, Syk could be overactivated in neurons due to aberrant regulation of neuronal excitability transmitted by non-TREM2/DAP12 signaling pathways in NHD brains.

Syk is dephosphorylated by specific protein-tyrosine phosphatases (PTPs).[33] Syk serves as a target for the Cbl-mediated ubiquitylation and degradation.[34] Thus, the biological activity of Syk in neurons is regulated at multiple levels by a delicate balance among phosphorylation, dephosphorylation and ubiquitylation. Finally, by bioinformatics analysis using KeyMolnet, a tool for analyzing molecular interactions on the comprehensive knowledgebase,[35] we found that Syk acts as a central player in the molecular network by connecting to 138 surrounding molecules (Fig. 5). Therefore, aberrant regulation of Syk activation affects diverse signals essential for various neuronal functions, possibly serving as a molecular basis for leukoencephalopathy in NHD, although the molecular link between a loss-of-function of TREM2/DAP12 and abnormal activation of Syk remains to be fully elucidated.

ACKNOWLEDGMENTS

REFERENCES

1. Nasu T, Tsukahara Y, Terayama K. A lipid metabolic disease – "Membranous lipodystrophy" – an autopsy case demonstrating numerous peculiar membrane-structures composed of compound lipid in bone and bone marrow and various adipose tissues. *Acta Pathol Jpn* 1973; **23**: 539–558.
2. Hakola HP. Neuropsychiatric and genetic aspects of a new hereditary disease characterized by progressive dementia and lipomembranous polycystic osteodysplasia. *Acta Psychiatr Scand Suppl* 1972; **232**: 1–173.
3. Bianchin MM, Capella HM, Chaves DL *et al.* Nasu-Hakola disease (polycystic lipomembranous osteodysplasia with sclerosing leukoencephalopathy – PLOSL): a dementia associated with bone cystic lesions. From clinical to genetic and molecular aspects. *Cell Mol Neurobiol* 2004; **24**: 1–24.
4. Tanaka J. Nasu-Hakola disease: a review of its leukoencephalopathic and membranolipodystrophic features. *Neuropathology* 2000; **20**: S25–S29.
5. Paloneva J, Manninen T, Christman G *et al.* Mutations in two genes encoding different subunits of a receptor signaling complex result in an identical disease phenotype. *Am J Hum Genet* 2002; **71**: 656–662.
6. Klünemann HH, Ridha BH, Magy L *et al.* The genetic causes of basal ganglia calcification, dementia, and bone cysts: DAP12 and TREM2. *Neurology* 2005; **64**: 1502–1507.
7. Ivashkiv LB. Cross-regulation of signaling by ITAM-associated receptors. *Nat Immunol* 2009; **10**: 340–347.
8. Lanier LL. DAP10- and DAP12-associated receptors in innate immunity. *Immunol Rev* 2009; **227**: 150–160.
9. Sada K, Takano T, Yanagi S, Yamamura H. Structure and function of Syk protein-tyrosine kinase. *J Biochem* 2001; **130**: 177–186.
10. Mócsai A, Ruland J, Tybulewicz VL. The SYK tyrosine kinase: a crucial player in diverse biological functions. *Nat Rev Immunol* 2010; **10**: 387–402.
11. Kaifu T, Nakahara J, Inui M *et al.* Osteopetrosis and thalamic hypomyelinosis with synaptic degeneration in DAP12-deficient mice. *J Clin Invest* 2003; **111**: 323–332.
12. Roumier A, Béchade C, Poncer JC *et al.* Impaired synaptic function in the microglial KARAP/DAP12-deficient mouse. *J Neurosci* 2004; **24**: 11421–11428.
13. Nataf S, Anginot A, Vuaillat C *et al.* Brain and bone damage in KARAP/DAP12 loss-of-function mice correlate with alterations in microglia and osteoclast lineages. *Am J Pathol* 2005; **166**: 275–286.

14. Otero K, Turnbull IR, Poliani PL *et al*. Macrophage colony-stimulating factor induces the proliferation and survival of macrophages via a pathway involving DAP12 and beta-catenin. *Nat Immunol* 2009; **10**: 734–743.

15. Takahashi K, Rochford CD, Neumann H. Clearance of apoptotic neurons without inflammation by microglial triggering receptor expressed on myeloid cells-2. *J Exp Med* 2005; **201**: 647–657.

16. Satoh JI, Tabunoki H, Ishida T *et al*. Immunohistochemical characterization of microglia in Nasu-Hakola disease brains. *Neuropathology* 2011; **31**: 363–375.

17. Zhang J, Billingsley ML, Kincaid RL, Siraganian RP. Phosphorylation of Syk activation loop tyrosines is essential for Syk function. An in vivo study using a specific anti-Syk activation loop phosphotyrosine antibody. *J Biol Chem* 2000; **275**: 35442–35447.

18. Mócsai A, Humphrey MB, Van Ziffle JA *et al*. The immunomodulatory adapter proteins DAP12 and Fc receptor γ-chain (FcRγ) regulate development of functional osteoclasts through the Syk tyrosine kinase. *Proc Natl Acad Sci U S A* 2004; **101**: 6158–6163.

19. Hamerman JA, Ni M, Killebrew JR, Chu CL, Lowell CA. The expanding roles of ITAM adapters FcRγ and DAP12 in myeloid cells. *Immunol Rev* 2009; **232**: 42–58.

20. Park H, Cox D. Syk regulates multiple signaling pathways leading to CX3CL1 chemotaxis in macrophages. *J Biol Chem* 2011; **286**: 14762–14769.

21. Zhou F, Hu J, Ma H, Harrison ML, Geahlen RL. Nucleocytoplasmic trafficking of the Syk protein tyrosine kinase. *Mol Cell Biol* 2006; **26**: 3478–3491.

22. Satoh J, Tabunoki H, Arima K. Molecular network analysis suggests aberrant CREB-mediated gene regulation in the Alzheimer disease hippocampus. *Dis Markers* 2009; **27**: 239–252.

23. Yanagi S, Inatome R, Takano T, Yamamura H. Syk expression and novel function in a wide variety of tissues. *Biochem Biophys Res Commun* 2001; **288**: 495–498.

24. Tsujimura T, Yanagi S, Inatome R *et al*. Syk protein-tyrosine kinase is involved in neuron-like differentiation of embryonal carcinoma P19 cells. *FEBS Lett* 2001; **489**: 129–133.

25. Hatterer E, Benon A, Chounlamountri N *et al*. Syk kinase is phosphorylated in specific areas of the developing nervous system. *Neurosci Res* 2011; **70**: 172–182.

26. Negro A, Brunati AM, Donella-Deana A, Massimino ML, Pinna LA. Multiple phosphorylation of α-synuclein by protein tyrosine kinase Syk prevents eosin-induced aggregation. *Faseb J* 2002; **16**: 210–212.

27. Lebouvier T, Scales TM, Hanger DP *et al*. The microtubule-associated protein tau is phosphorylated by Syk. *Biochim Biophys Acta* 2008; **1783**: 188–192.

28. Hirose M, Kitano J, Nakajima Y *et al*. Phosphorylation and recruitment of Syk by immunoreceptor tyrosine-based activation motif-based phosphorylation of tamalin. *J Biol Chem* 2004; **279**: 32308–32315.

29. Kerrigan AM, Brown GD. Syk-coupled C-type lectin receptors that mediate cellular activation via single tyrosine based activation motifs. *Immunol Rev* 2010; **234**: 335–352.

30. Shefler I, Sagi-Eisenberg R. Gi-mediated activation of the Syk kinase by the receptor mimetic basic secretagogues of mast cells: role in mediating arachidonic acid/metabolites release. *J Immunol* 2001; **167**: 475–481.

31. Takano T, Sada K, Yamamura H. Role of protein-tyrosine kinase syk in oxidative stress signaling in B cells. *Antioxid Redox Signal* 2002; **4**: 533–541.

32. Gao J, Zoller KE, Ginsberg MH, Brugge JS, Shattil SJ. Regulation of the pp72syk protein tyrosine kinase by platelet integrin αIIbβ3. *EMBO J* 1997; **16**: 6414–6425.

33. Tsang E, Giannetti AM, Shaw D *et al*. Molecular mechanism of the Syk activation switch. *J Biol Chem* 2008; **283**: 32650–32659.

34. Rao N, Ghosh AK, Ota S *et al*. The non-receptor tyrosine kinase Syk is a target of Cbl-mediated ubiquitylation upon B-cell receptor stimulation. *EMBO J* 2001; **20**: 7085–7095.

35. Satoh J. Bioinformatics approach to identifying molecular biomarkers and networks in multiple sclerosis. *Clin Exp Neuroimmunol* 2010; **1**: 127–140.
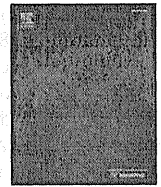
Review

Molecular network of microRNA targets in Alzheimer's disease brains

Jun-ichi Satoh *

Department of Bioinformatics and Molecular Neuropathology, Meiji Pharmaceutical University, 2-522-1 Noshio, Kiyose, Tokyo 204-8588, Japan

ABSTRACT

MicroRNAs (miRNAs) are a group of small noncoding RNAs that regulate translational repression of target mRNAs. The vast majority of presently identified miRNAs are expressed in the brain where they fine-tune the expression of a wide range of target molecules essential for neuronal and glial development, differentiation, proliferation, apoptosis and metabolism. Aberrant expression and dysfunction of brain-enriched miRNAs induce development of neurodegenerative diseases, such as Alzheimer's disease (AD) and Parkinson's disease (PD). Because a single miRNA concurrently downregulates hundreds of target mRNAs, the set of miRNA target genes coregulated by an individual miRNA generally constitutes the biologically integrated network of functionally associated molecules. Recent advances in systems biology enable us to characterize the global molecular network of experimentally validated targets for individual miRNAs by using pathway analysis tools of bioinformatics endowed with comprehensive knowledgebase. This review is conducted to summarize accumulating studies focused on aberrant miRNA expression in AD brains, and to propose the systems biological view that abnormal regulation of cell cycle progression as a result of deregulation of miRNA target networks plays a central role in the pathogenesis of AD.

© 2011 Published by Elsevier Inc.

Contents

Introduction

MicroRNAs (miRNAs) constitute a class of endogenous small non-coding RNAs that mediate posttranscriptional regulation of protein-coding genes by binding mainly to the 3' untranslated region (3' UTR) of target mRNAs, leading to translational inhibition, mRNA destabilization or degradation, depending on the degree of sequence complementarity. During their biogenesis, the primary miRNAs (pri-miRNAs) are transcribed from the intra- and inter-genic regions of the genome by RNA polymerase II, and processed by the RNase III enzyme Drosha into pre-miRNAs. After nuclear export, they are processed by RNase III enzyme Dicer into mature miRNAs consisting of approximately 22 nucleotides. Finally, a single-stranded miRNA is loaded onto the RNA-induced silencing complex (RISC), where the seed sequence located at positions 2 to 8 from the 5' end of the miRNA plays a crucial role in recognition of the target mRNA.

At present, more than one thousand of human miRNAs are registered in miRBase Release 17 (April 2011; www.mirbase.org). A single miRNA capable of binding to numerous target mRNAs concurrently reduces production of hundreds of proteins, whereas the 3'UTR of a single mRNA is often targeted by multiple different miRNAs, providing the complexity of miRNA-regulated gene expression (Filipowicz et al., 2008; Selbach et al., 2008). Consequently, the whole human miRNA system (microRNAome) regulates greater than 60% of all protein-coding genes essential for cellular development, differentiation, proliferation, apoptosis and metabolism (Friedman et al., 2009). Approximately 70% of presently identified miRNAs are expressed in the brain in a spatially and temporally controlled manner, where they fine-tune diverse neuronal and glial functions (Fineberg et al., 2009). Actually, aberrant expression and dysfunction of brain-enriched miRNAs induce development of neurodegenerative diseases, such as Alzheimer's disease (AD) and Parkinson's disease

* Corresponding author. Fax: +81 42 495 8678.
  E-mail address: satoj@my-pharm.ac.jp.

(PD) (Harraz et al., in press; Kocerha et al., 2009; Maes et al., 2009; Nelson et al., 2008).

Recent advances in systems biology have made major breakthroughs by illustrating the cell-wide map of complex molecular interactions with the aid of the literature-based knowledgebase of molecular pathways (Viswanathan et al., 2008). The logically arranged molecular networks construct the whole system characterized by robustness that maintains the proper function of the system in the face of genetic and environmental perturbations (Kitano, 2007). In the scale-free molecular network, targeted disruption of several critical components designated hubs, on which the biologically important molecular interactions concentrate, efficiently disturbs the whole cellular function by destabilizing the network (Albert et al., 2000). From the point of view of the molecular network constructed by target genes for a particular miRNA, the identification and characterization of the hub would help us to understand biological and pathological roles of the individual miRNA. By combining the application of the miRNA target prediction program TargetScan and the Human Protein Reference Database (HPRD), a recent study investigated the global human microRNA-regulated protein–protein interaction (PPI) network (Hsu et al., 2008). Importantly, individual miRNAs often target the hub itself within the PPI network.

AD is the most common cause of dementia worldwide, affecting the elderly population, characterized by the hallmark pathology of amyloid-β (Aβ) deposition, neurofibrillary tangle (NFT) formation, and extensive neuronal degeneration in the brain. Aβ is derived from the sequential cleavage of amyloid precursor protein (APP) by beta-site APP-cleaving enzyme 1 (BACE1) and the γ-secretase complex. Although the precise pathological mechanisms underlying AD remain largely unknown, accumulating evidence indicates that aberrant regulation of miRNA-dependent gene expression is closely associated with molecular events responsible for Aβ production, NFT formation, and neurodegeneration (Hébert et al., 2008, 2010; Wang et al., 2008, 2011). The aim of the present study is to review recent studies focused on aberrant miRNA expression in AD brains, and to propose the systems biological view that deregulation of miRNA target networks plays a central role in the pathogenesis of AD.

Aberrant miRNA expression in AD brains

Increasing evidence indicates that deregulation of miRNA expression plays a key role in AD pathogenesis, as a recent review indicated (Table 1 modified from Satoh, 2010). The pioneering work identified upregulated expression of miR-9 and miR-128 in the hippocampus of AD brains by using a nylon membrane-bound DNA array (Lukiw, 2007). More recently, the same group showed that the levels of expression of miR-146a are elevated in the hippocampus and the superior temporal cortex of AD patients (Lukiw et al., 2008). Importantly, nuclear factor-kappa B (NF-κB), a transcription factor indispensable for diverse immune responses, regulates the expression of miR-146a that targets complement factor H (CFH) and IL-1 receptor-associated kinase-1 (IRAK1), leading to sustained inflammation in AD brains where the expression of NF-κB is also upregulated (Cui et al., 2010; Lukiw et al., 2008). Furthermore, they clarified the limited stability of brain-enriched miRNAs composed of a high content of AU and UA dinucleotides (Sethi and Lukiw, 2009).

A different group showed that miR-107 targets BACE1, a rate-limiting enzyme for Aβ production (Wang et al., 2008). By analyzing a miRNA microarray, they found that miR-107 levels are substantially reduced in the temporal cortex not only of AD but also of the patients affected with mild cognitive impairment (MCI), indicating that downregulation of miR-107 begins at the very early stage of AD. More recently, they validated a negative correlation between miR-107 levels and the amounts of neuritic plaques and NFTs in the temporal cortex of AD patients by quantitative RT-PCR (qRT-PCR) (Nelson and Wang, 2010). The levels of miR-107 and miR-103, both of which target the

actin-binding protein cofilin, are reduced in the brains of Tg19959 mice overexpressing human APP carrying the KM670/671NL and V717F familial AD mutations (Yao et al., 2010). These observations are responsible for formation of rod-like aggregates of cofilin in brains of a transgenic mouse model of AD.

By using a miRNA microarray, a previous study identified reduced expression of the miR-29a/b-1 cluster, inversely correlated with BACE1 protein levels, in the anterior temporal cortex of AD patients (Hébert et al., 2008). The miRNA target database search predicted the presence of binding sites in the human BACE1 mRNA 3′UTR for miR-9, 15a, 19b, and 29a/b-1 and in the human APP mRNA 3′UTR for let-7, miR-15a, 101, and 106b, all of which are downregulated in AD brains. Actually, the introduction of pre-miR-29 reduces secretion of Aβ from HEK293 cells stably expressing the APP Swedish (APPswe) mutation (Hébert et al., 2008). Later, they identified reduced expression of miR-106b that targets APP in the anterior temporal cortex of AD patients (Hébert et al., 2009).

The levels of miR-298 and miR-328, both of which target mouse BACE1, are reduced in the hippocampus of aged APPswe/PS1 (A246E) transgenic mice (Boissonneault et al., 2009). In contrast, the levels of a noncoding BACE1-antisense (BACE1-AS) RNA that enhances BACE1 mRNA stability are elevated in the brains of Tg19959 APP transgenic mice (Faghihi et al., 2008). BACE1-AS masks the miR-485-5p binding site located within the open-reading frame of BACE1 mRNA, and thereby inhibits miR-485-5p-mediated repression of BACE1 mRNA translation (Faghihi et al., 2010). Actually, the levels of expression of miR-485-5p are reduced but those of BACE1-AS are elevated in the entorhinal cortex and the hippocampus of AD patients. In cultured rat hippocampal neurons, a brain-enriched microRNA miR-101 acts as a negative regulator of APP expression by binding to the APP 3′UTR (Vilardo et al., 2010).

All of these observations suggest the concept that abnormal repression of a battery of miRNAs accelerates Aβ production via overexpression of BACE1, the enzyme and/or APP, the substrate in AD brains. However, the genetic variability of miRNA-binding sites in both BACE1 and APP mRNA 3′UTRs does not confer a risk factor for development of AD (Bettens et al., 2009). It sounds reasonable, because miRNAs in general induce translational inhibition without requiring the perfect match of binding sequences in target mRNAs. It is worthy to note that a neuron-specific microRNA miR-124, downregulated in the anterior temporal cortex of AD brains, targets polypyrimidine tract binding protein 1 (PTBP1), a global repressor of alternative pre-mRNA splicing (Smith et al., 2011). Upregulation of PTBP1 induces the inclusion of APP exons 7 and 8, suggesting a novel role of miRNAs in neuronal splicing regulation of APP.

By qRT-PCR and luciferase reporter assay, we found that miR-29a, whose levels are decreased in the frontal cortex of AD brains, targets neuron navigator 3 (NAV3) (Shioya et al., 2010). NAV3 immunoreactivity was greatly enhanced in NFT-bearing pyramidal neurons in the cerebral cortex of AD brains. Although the precise biological function of the human NAV3 protein remains unknown, the *Caenorhabditis elegans* homolog regulates axon guidance (Maes et al., 2002), suggesting that our findings reflect a neuronal compensatory response against NFT-generating neurodegenerative events. The conditional deletion of Dicer, a master regulator of miRNA processing, induces neurodegeneration accompanied by hyperphosphorylation of tau in the adult mouse forebrain and the hippocampus (Hébert et al., 2010). They identified extracellular signal-regulated kinase 1 (ERK1) regulated by the miR-15 family as a candidate kinase responsible for tau phosphorylation. The levels of miR-15a are substantially reduced in AD brains.

By qRT-PCR, a previous study characterized miRNA expression profiles of the brain and cerebrospinal fluid (CSF) samples isolated from AD patients and non-demented controls (Cogswell et al., 2008). Among a panel of miRNAs either upregulated or downregulated in the hippocampus, the medial frontal cortex, and the cerebellum of AD patients, they identified a close relationship between upregulated miRNAs and metabolic pathways, including insulin signaling, glycolysis, and

Table 1
Aberrant expression of miRNAs in AD brains.

Authors and years	Patients and brain regions	Methods for miRNA expression profiling	Aberrantly expressed miRNAs	Upregulation or downregulation	Target mRNAs characterized	Target prediction and validation	Possible pathological implications
Lukiw (2007)	5 AD patients and 5 age-matched controls; the hippocampus	Northern blot	miR-9, miR-128	Up	ND	ND	General neuropathology of AD
Lukiw et al. (2008)	23 AD patients and 23 age-matched controls; the hippocampus and the superior temporal lobe neocortex	Microarray, northern blot	miR-146a	Up	CFH	ND; knockdown of miR-146a	Sustained inflammatory responses
Wang et al. (2008)	6 AD and 6 MCI patients and 11 non-demented controls; the temporal cortex	Microarray, northern blot, ISH	miR-107	Down	BACE1	miRanda, TargetScan, PicTar; luciferase reporter assay	Increased production of Ab
Hébert et al. (2008)	5 AD patients and 5 age-matched controls; the anterior temporal cortex	Microarray, qRT-PCR	miR-29a/b-1	Down	BACE1	miRanda, TargetScan, Pictar, miRBase; luciferase reporter assay	Increased production of Ab
			miR-15a, miR-9, miR-19b	Down	BACE1	miRanda, TargetScan, Pictar, miRBase; not validated	
			let-7i, miR-15a, miR-101, miR-106b	Down	APP	miRanda, TargetScan, Pictar, miRBase; not validated	
			miR-22, miR-26b, miR-93, miR-181c, miR-210, miR-363	Down	ND	ND	
			miR-197, miR-511, miR-320	Up	ND	ND	
Cogswell et al. (2008)	15 AD patients and 12 non-demented controls; the cerebellum	qRT-PCR	miR-27a, miR-27b, miR-34a, miR-100, miR-125b, miR-381, miR-422a	Up	ND	miRanda, RNAhybrid; not validated	General neuropathology of AD
			miR-9, miR-98, miR-132, miR-146b, miR-212, miR-425	Down	ARHGAP32 for miR-132		
	15 AD patients and 12 non-demented controls; the hippocampus		miR-26a, miR-27a, miR-27b, miR-30e-5p, miR-34a, miR-92, miR-125b, miR-145, miR-200c, miR-381, miR-422a, miR-423	Up	ND		
			miR-9, miR-30c, miR-132, miR-146b, miR-210, miR-212, miR-425	Down	ARHGAP32 for miR-132		
	15 AD patients and 12 non-demented controls; the medial frontal gyrus		miR-27a, miR-27b, miR-29a, miR-29b, miR-30c, miR-30e-5p, miR-34a, miR-92, miR-100, miR-125b, miR-145, miR-148a, miR-381, miR-422a, miR-423	Up	ND		
			miR-9, miR-26a, miR-132, miR-146b, miR-200c, miR-210, miR-212, miR-425	Down	ARHGAP32 for miR-132		
Hébert et al. (2009)	19 AD patients and 11 non-demented controls; the anterior temporal cortex	qRT-PCR	miR-106b	Down	APP	miRanda, TargetScan, Pictar, miRBase; luciferase reporter assay	Increased production of Ab
Sethi and Lukiw (2009)	6 AD and 13 non-AD patients and 6 controls; the temporal lobe cortex	Microarray, northern blot	miR-9, miR-125b, miR-146a	Up	ND	ND	General neuropathology of AD
Nunez-Iglesias et al. (2010)	5 AD patients and 5 age-matched controls; the parietal lobe cortex	Microarray	miR-18b, miR-34c, miR-615, miR-629, miR-637, miR-657, miR-661, mir-09369, mir-15903, mir-44691	Nd	positively correlated with target mRNAs	miRanda, TargetScan, PicTar; not validated	General neuropathology of AD
			miR-211, miR-216, miR-325, miR-506, miR-515-3p, miR-612, miR-768-3p, mir-06164, mir-32339, mir-45496	Nd	negatively correlated with target mRNAs	miRanda, TargetScan, PicTar; not validated	
Shioya et al. (2010)	7 AD patients and 4 non-neurological controls; the frontal lobe	qRT-PCR	miR-29a	Down	NAV3	TargetScan, Pictar, miRBase; luciferase reporter assay	A putative compensatory mechanism

3

Table 1 (*continued*)

Authors and years	Patients and brain regions	Methods for miRNA expression profiling	Aberrantly expressed miRNAs	Upregulation or downregulation	Target mRNAs characterized	Target prediction and validation	Possible pathological implications
							against neurodegenerative events
Hébert et al. (2010)	8 AD patients and 10 non-demented patients; the anterior temporal cortex	qRT-PCR	miR-15a	Down	ERK1	TargetScan, miRanda; overexpression or knockdown of miR-15a, luciferase reporter assay	Hyperphosphorylation of tau
Cui et al. (2010)	36 AD patients and 30 age-matched controls; the hippocampus and the superior temporal lobe neocortex	Microarray, northern blot	miR-146a	Up	IRAK1	miRBase; knockdown of miR-146a	Sustained inflammatory responses
Faghihi et al. (2010)	35 AD patients and 35 normal elderly controls; the entorhinal cortex and the hippocampus	qRT-PCR	miR-485-5p	Down	BACE1	miRanda; luciferase reporter assay	increased production of Ab
Smith et al. (2011)	11 AD patients and 11 non-demented patients; the anterior temporal cortex	qRT-PCR	miR-124	Down	PTBP1	known target previously validated by luciferase reporter assay	Aberrant APP mRNA alternative splicing
Wang et al. (2011)	10 elderly females with various pathological stages of AD; the gray matter and the white matter of the superior and middle temporal cortex	Microarray, northern blot	miR-519e, miR-574-5p, miR-498, miR-518a-5p/miR-527, miR-525-5p, miR-300, miR-576-3p, miR-583, miR-146b-3p, miR-490-3p, miR-549, miR-516a-5p, miR-510, miR-184, miR-516b, miR-298, miR-214, miR-198, miR-451, miR-144, miR-424, let-7e	Up in the gray matter (group A)	ND	ND	General neuropathology of AD
			miR-509-5p, miR-574-3p, miR-576-5p, miR-302e, miR-220b, miR-208a, miR-215	Up in the white matter (group B)			
			miR-485-3p, miR-381, miR-124, miR-34a, miR-129-5p, miR-29a, miR-143, miR-136, miR-145, miR-138, miR-129-3p, miR-128, miR-379, miR-299-5p, miR-218, miR-149, miR-135a, miR-7, miR-126, miR-411, miR-335, miR-9, miR-378, miR-488, miR-432,	Down in the gray matter (group C)			

ARTICLE IN PRESS

miR-127-5p, miR-127-3p, miR-491-5p, miR-376c, miR-377, miR-95, miR-222, miR-29b, miR-329, miR-495, miR-551b, miR-195, miR-125b, miR-30b, miR-221, miR-139-5p, miR-487a, miR-487b, miR-107, miR-146b-5p, miR-29c, miR-30a, miR-582-5p, miR-103, miR-342-3p, miR-331-3p, miR-30c, miR-30d, miR-382, miR-22, miR-125a-5p miR-491-3p, miR-423-5p, miR-34b, miR-422a, miR-34c-5p, miR-584, miR-219-5p, miR-338-3p, miR-219-2-3p, miR-338-5p, miR-181a, miR-181b, let-7b, miR-151-3p, miR-197, miR-19a, miR-20a, miR-17, miR-106a, miR-32, miR-340, miR-19b, miR-21, miR-151-5p, miR-194, let-7c, miR-330-3p, miR-27b, miR-93, miR-15a, miR-339-5p, miR-193b, miR-106b, miR-16, miR-23b, miR-15b, miR-320d, miR-320b, miR-320c, miR-320a, miR-557, miR-33a, let-7a, miR-374b, miR-140-3p, miR-374a, miR-24, miR-140-5p, miR-26a, miR-513a-5p, miR-212, miR-142-5p, miR-142-3p, miR-26b, miR-520d-5p, miR-193a-3p, miR-92b, miR-330-5p, miR-186, let-7f, miR-223, miR-412, miR-185, miR-148b, miR-101, miR-99b, miR-27a, miR-589, let-7i, miR-361-3p, miR-361-5p, miR-423-3p, miR-190, miR-301a, miR-365, miR-23a, miR-363, miR-326 miR-425, miR-191, miR-519d, let-7 g, miR-98, miR-99a, miR-30e	Down in the white matter (group D) Down in the gray matter (group E)	

The table is modified from that of the recent review article with permission of reproduction (Satoh, 2010). Abbreviations: AD, Alzheimer disease; MCI, mild cognitive impairment; qRT-PCR, quantitative RT-PCR; ISH, in situ hybridization; BACE1, beta-site APP-cleaving enzyme 1; APP, amyloid precursor protein; Ab, amyloid-beta; CFH, complement factor H; NAV3, neuron navigator 3; ERK1, extracellular signal-regulated kinase 1; ARHGAP32, Rho GTPase activating protein 32 (p250GAP); IRAK1, IL-1 receptor-associated kinase-1; PTBP1, polypyrimidine tract binding protein 1; and ND, not determined.

glycogen metabolism. Furthermore, they found that the levels of all miR-30 family members are elevated in CSF samples of AD patients. Because circulating miRNAs in the plasma serve as a biomarker for diagnosis and prediction of prognosis of human cancers (Mitchell et al., 2008), the identification of AD-specific miRNAs in the serum and the CSF would be a worthwhile project in the future.

By combining microarray-based miRNA expression profiling and genome-wide transcriptome analysis of the brains of AD patients and age-matched controls, a recent study showed that the levels of several miRNAs are not only negatively but also positively correlated with those of potential target mRNAs (Nunez-Iglesias et al., 2010). The expression of miR-211 shows a negative correlation with mRNA levels of BACE1, RAB43, LMNA, MAP2K7, and TADA2L, whereas the expression of mir-44691 exhibits a positive correlation with mRNA levels of CYR61, CASR, POU3F2, GGPR68, DPF3, STK38, and BCL2L2 in AD brains. Although a previous study showed that certain miRNAs exceptionally activate transcription and translation of targets (Vasudevan et al., 2007), the direct interaction between mir-44691 and their targets requires further investigation and validation.

Thus, different studies identified aberrant expression of distinct miRNAs in AD brains. This variability is mostly attributable to disease-specific and nonspecific interindividual differences, including differences in age, sex, genetic background, the brain region, the pathological stage, and the postmortem interval (PMI), because most studies include fairy limited numbers of patients' samples and controls, which are often complicated by variable confounding factors (Table 1). Importantly, distinct populations of neurons in different cerebral cortical layers express a discrete set of miRNAs in the human transentorhinal cortex (Nelson et al., 2010).

MicroRNA target networks suggest the involvement of deregulation of cell cycle progression in AD pathogenesis

Because a single miRNA concurrently downregulates hundreds of target mRNAs, the set of miRNA target genes coregulated by an individual miRNA generally constitutes the biologically integrated network of functionally associated molecules (Hsu et al., 2008; Satoh and Tabunoki, 2011). Even small changes in the expression level of a single miRNA could affect a wide range of signaling pathways involved in diverse biological functions. From this point of view, the characterization of a global picture of miRNA target networks would promote us to understand miRNA-mediated molecular mechanisms underlying AD.

To identify biologically relevant molecular networks from the large-scale data, we could analyze them by using a battery of pathway analysis tools of bioinformatics endowed with comprehensive knowledgebase, such as Kyoto Encyclopedia of Genes and Genomes (KEGG) (Kanehisa et al., 2010; www.kegg.jp), Ingenuity Pathways Analysis (IPA) (Ingenuity Systems; www.ingenuity.com), and KeyMolnet (Institute of Medicinal Molecular Design; www.immd.co.jp). KEGG is a public database, while both IPA and KeyMolnet are commercial ones. KEGG includes manually curated reference pathways that cover a wide range of metabolic, genetic, environmental, and cellular processes, and human diseases. Currently, KEGG contains 134,511 distinct pathways generated from 391 reference pathways.

IPA is a knowledgebase that contains approximately 2,270,000 biological and chemical interactions and functional annotations with definite scientific evidence, curated by expert biologists. By uploading the list of Gene IDs and expression values, the network-generation algorithm identifies focused genes integrated in a global molecular network. IPA calculates the score p-value that reflects the statistical significance of association between the genes and the networks by the Fisher's exact test.

KeyMolnet contains knowledge-based contents on 131,000 relationships among human genes and proteins, small molecules, diseases, pathways and drugs, curated by expert biologists (Satoh et al., 2009). They are categorized into the core contents collected from selected review articles with the highest reliability or the secondary contents

Table 2
Gene ontology terms of target genes for miRNAs downregulated in AD brains.

Rank	GO term	The number of genes in the term	Bonferroni corrected p-value
1	GO:0042127 – regulation of cell proliferation	126	3.37E-25
2	GO:0043067 – regulation of programmed cell death	119	4.03E-20
3	GO:0010941 – regulation of cell death	119	5.55E-20
4	GO:0042981 – regulation of apoptosis	117	1.88E-19
5	GO:0043069 – negative regulation of programmed cell death	69	1.88E-16
6	GO:0051094 – positive regulation of developmental process	60	2.01E-16
7	GO:0060548 – negative regulation of cell death	69	2.20E-16
8	GO:0045597 – positive regulation of cell differentiation	54	2.80E-16
9	GO:0043066 – negative regulation of apoptosis	68	3.75E-16
10	GO:0010604 – positive regulation of macromolecule metabolic process	114	1.00E-15
11	GO:0008284 – positive regulation of cell proliferation	73	2.13E-15
12	GO:0051726 – regulation of cell cycle	61	4.12E-13
13	GO:0012501 – programmed cell death	87	8.24E-13
14	GO:0031328 – positive regulation of cellular biosynthetic process	93	1.24E-12
15	GO:0006357 – regulation of transcription from RNA polymerase II promoter	96	2.47E-12
16	GO:0009891 – positive regulation of biosynthetic process	93	3.71E-12
17	GO:0010033 – response to organic substance	95	4.53E-12
18	GO:0051174 – regulation of phosphorus metabolic process	74	5.36E-12
19	GO:0019220 – regulation of phosphate metabolic process	74	5.36E-12
20	GO:0042325 – regulation of phosphorylation	72	7.00E-12

The list of 852 target genes for the set of miRNAs downregulated in AD brains was imported into the Functional Annotation tool of DAVID. The top 20 GO terms showing a significant association with target genes are listed with rank, GO term, the number of genes in the term, and p-value following Bonferroni correction.

Table 3
KEGG pathways of target genes for miRNAs downregulated in AD brains.

Rank	KEGG pathway	The number of genes in the pathway	Bonferroni corrected p-value
1	hsa05200:Pathways in cancer	81	3.16E-21
2	hsa05220:Chronic myeloid leukemia	32	3.77E-14
3	hsa05212:Pancreatic cancer	30	7.55E-13
4	hsa05219:Bladder cancer	23	2.00E-12
5	hsa05215:Prostate cancer	32	9.63E-12
6	hsa05222:Small cell lung cancer	28	3.81E-09
7	hsa05210:Colorectal cancer	27	2.35E-08
8	hsa05223:Non-small cell lung cancer	21	9.28E-08
9	hsa05218:Melanoma	24	1.02E-07
10	hsa04110:Cell cycle	32	1.92E-07
11	hsa04510:Focal adhesion	42	2.35E-07
12	hsa04012:ErbB signaling pathway	26	3.12E-07
13	hsa05214:Glioma	22	3.23E-07
14	hsa05213:Endometrial cancer	20	3.32E-07
15	hsa05211:Renal cell carcinoma	21	1.52E-05
16	hsa04115:p53 signaling pathway	20	4.75E-05
17	hsa05221:Acute myeloid leukemia	18	9.63E-05
18	hsa04010:MAPK signaling pathway	43	3.40E-04
19	hsa04914:Progesterone-mediated oocyte maturation	21	5.61E-04
20	hsa04350:TGF-beta signaling pathway	21	6.79E-04

The list of 852 target genes for the set of miRNAs downregulated in AD brains was imported into the Functional Annotation tool of DAVID. The top 20 KEGG pathways showing a significant association with target genes are listed with rank, KEGG pathway, the number of genes in the pathway, and p-value following Bonferroni correction. The molecular pathway entitled "hsa04110:Cell cycle" (Rank 10) is illustrated in Fig. 1.
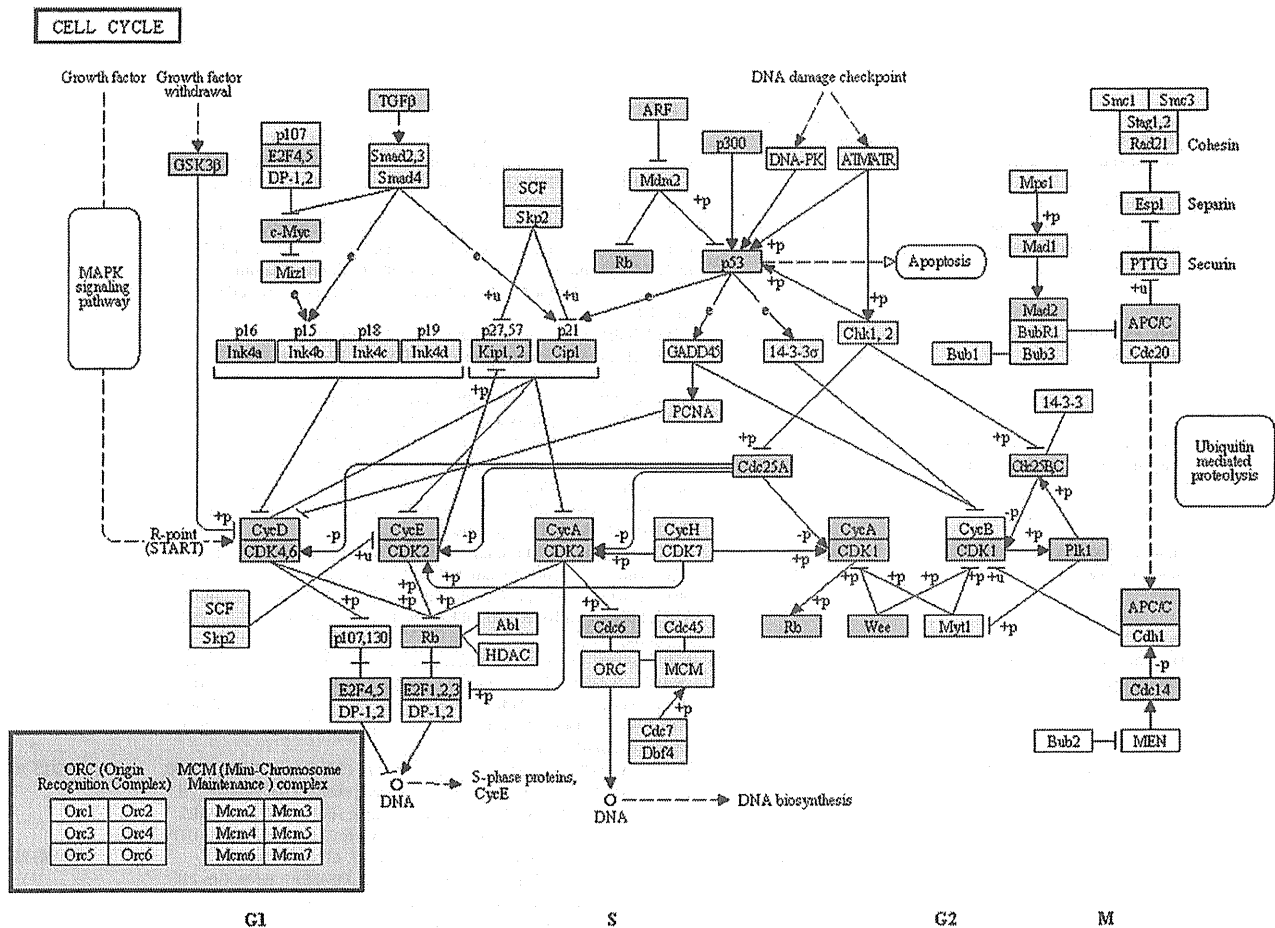
Fig. 1. Target genes for miRNAs downregulated in AD brains are located in the cell cycle pathway of KEGG. The list of 852 target genes for the set of miRNAs downregulated in AD brains (Supplementary Table 1) was imported into the Functional Annotation tool of DAVID. Among the top 20 KEGG pathways showing a significant association with target genes, the molecular pathway entitled "hsa04110:Cell cycle" (Rank 10 in Table 3) is illustrated. Target genes highlighted by pink are potentially upregulated in AD brains.

extracted from abstracts of PubMed and HPRD. By uploading the list of Gene IDs, KeyMolnet automatically provides corresponding molecules and a minimum set of intervening molecules as a node on networks. The "neighboring" network-search algorithm selected one or more molecules as starting points to generate the network of all kinds of molecular interactions around starting molecules, including direct activation/inactivation, transcriptional activation/repression, and the complex formation within the designated number of paths from starting points. The generated network was compared side by side with 443 human canonical pathways of the KeyMolnet library. The algorithm counting the number of overlapping molecular relations between the extracted network and the canonical pathway makes it possible to identify the canonical pathway showing the most significant contribution to the extracted network. The significance in the similarity between both is scored following the formula, where O = the number of overlapping molecular relations between the extracted network and the canonical pathway, V = the number of molecular relations located in the extracted network, C = the number of molecular relations located in the canonical pathway, T = the number of total molecular relations, and the x = the sigma variable that defines coincidence.

$$Score = -\log_2(Score(p)) \qquad Score(p) = \sum_{x=0}^{Min(C,V)} f(x) \qquad f(x)$$

$$= {}_C C_x \cdot {}_{T-C} C_{V-x} / {}_T C_V.$$

In the present study, we attempted to characterize the networks of target genes for a battery of miRNAs aberrantly expressed in AD brains. For this purpose, we have focused on the currently available most comprehensive dataset of miRNA expression profiling of AD brains (Wang et al., 2011) (Table 1). This includes expression profiles of miRNAs isolated separately from the gray matter and the white matter of the superior and middle temporal cerebral cortex. All samples were taken within 4 h at PMI and processed for the rigid control of RNA quality. The samples were derived from control subjects with no AD pathology and the patients with the early AD pathology, evaluated by the density of diffuse plaques, neuritic plaques, and NFTs. Hierarchical clustering of expression profiles categorized AD-relevant 171 miRNAs into five groups tentatively named A to E, presenting with similar expression patterns within the group, either upregulated or downregulated in the gray matter or in the white matter of AD brains (Wang et al., 2011) (Table 1). Because the white matter is enriched in neuronal axons in which certain miRNAs are transported (Schratt et al., 2006), the white matter-enriched fraction does not exclude the inclusion of neuron-specific miRNAs. For simplicity, we combined the data of the white matter and the gray matter fractions, and separated them into two categories, such as the set of upregulated miRNAs consisting of groups A and B and the set of downregulated miRNAs consisting of groups C, D, and E.

Recently, various bioinformatics programs armed with distinct algorithms have been established for the in silico prediction of miRNA

Table 4

IPA functional networks of target genes for miRNAs downregulated in AD brains.

| Rank	IPA functional network	Molecules in the network	Fisher's test p-value
1	Cancer, dermatological diseases and conditions, cellular growth and proliferation	Ap1, BCL2, CAV1, CEBPA, CEP63, COMMD9, CTGF, ETS1, FGF2, GLI1, HRAS, Ige, JUN, KRAS, NFKB1, NIPAL2, Nos, OSBPL8, P38 MAPK, PAPSS2, PLAG1, PTGFRN, PTGS2, PXDN, SERBP1, SIGMAR1, SOX9, SP1, SP3, SPP1, SQSTM1, VDR, VEGFA, VIM, WT1	1.00E-43
2	Organ development, cellular development, nervous system development and function	ACTR8, ACVR1, ACVR1B, ADSS, Alp, ANKRD27, BMP, BMP7, BMPR2, BMPR1B, COL1A2, CSHL1, CTDSP1, CTDSP2, DLL1, GSK3B, HES1, ID2, ID3, IGF2BP1, KLF4, MIR24 (human), Notch, NOTCH1, NOTCH2, Pro-inflammatory Cytokine, RAB21, Smad, SMAD1, SMAD5, SOX2, TGFBR1, TGFBR2, UHMK1, ZBED3	1.00E-38
3	Gene expression, cell cycle, DNA replication, recombination, and repair	ASXL2, BMI1, BTG2, CBX7, CDCA4, CDK2-CyclinE, DHFR, DNA (cytosine-5-)-methyltransferase, DNMT1, DNMT3A, DNMT3B, E2F2, E2F3, E2F5, E2F6, ERK, EZH2, Gap, HELLS, JARID2, MIR101, MIR125B (human), MIR26A (human), MYT1, PHB, PHF19, RING1, SGPL1, SNAI2, SPRED1, TDG, Thymidine Kinase, TYMS, UHRF1, ZNF238	1.00E-34
4	Cell cycle, connective tissue development and function, cellular growth and proliferation	ARID4B, ARL2, AURKB, BRCA1, CA12, CCDC99, CCNT2, CDCA7L, CDKN2A, DKK1, DRAM1, E2F1, Ep300/Pcaf, ERH, EYA4, FAM3C, GTF2H1, Histone h4, Holo RNA polymerase II, P-TEFb, PERP, PRMT5, Rb, RNA polymerase II, RPA, RRP8, SIRT1, TAF9B, TARBP1, TMED2, TMED7, TMED10, TMEM43, TP53, TP53INP1	1.00E-33
5	Lipid metabolism, molecular transport, small molecule biochemistry	26s Proteasome, Alpha tubulin, ARIH2, ATXN1, CDC34, CDKAL1, FADS2, HARS, HMG CoA synthase, Ikb, IKK (complex), LASS2, MAN2A1, MAPK1IP1L, MDM4, NOVA1, ODZ2, PECI, PFK, PTEN, RAD23B, SLC25A1, SLC25A22, SNCA, SOX4, SRSF10, TUBB6, UBE2, Ube3, UBE2I, UBE2Q1, UBE2S, UBE2V1, Ubiquitin, UGP2	1.00E-31
6	Lipid metabolism, small molecule biochemistry, cell signaling	ACAA2, acetyl-CoA C-acyltransferase, ANXA8/ANXA8L1, Arginase, BACE1, BNIP3L, CASP6, CASP3/6/7, Cytokeratin, Fgfr, FMOD, FNDC3B, HADH, HADHB, Hspg, IMPDH1, Lamin, LMNB1, MBNL2, Mediator, Mhc class ii, MPHOSPH9, MTRR, NAT6, NUCB1, PGRMC1, PGRMC2, PNP, RBMS1, RPS7, SLC35A1, Tenascin, TGFB1, UGDH, VPS39	1.00E-30
7	Cell cycle, cell death, cancer	ABHD5, ADIPOR2, AP2A1, APC, APP, CDKN1A, CLDND1, ELMOD2, EP300, ERBB2, GLCCI1, Hemoglobin, HIF1A, HISTONE, Histone h3, HNRNPK, IL1, Insulin, LAMB3, LRRC8C, MAN1A1, MYC, Ndpk, NR3C1, PPARA, PPARG, RAB34, RAD51C, RB1, RELA, ROCK2, SLC38A1, SLC7A11, TNFRSF21, UTP15	1.00E-30
8	Cell-to-cell signaling and interaction, cellular growth and proliferation, connective tissue development and function	ATP2A2, BRAP, CCND1, CCND2, CCND3, CDCA7, CENPJ, CTNNBIP1, Cyclin D1/cdk4, EIF4A, EIF4A1, EIF4E, Eif4ebp, EIF4EBP1, Eif4g, Gm-csf, IDH1, IGF2, IGF2R, JAK2, KAT2B, LIF, MTPN, NR4A2, p70 S6k, Pdgf (complex), PDGF BB, PMS1, SKAP2, STAT, STAT5A, STAT5a/b, TGFB3, TUSC2, UAP1	1.00E-29
9	Cellular growth and proliferation, tumor morphology, cellular development	Adaptor protein 1, AFF1, AP1M2, Camk, CAMK2G, Creb, CREB1, DNAJ, DNAJB4, DNAJB11, DNAJC1, DNAJC27, Gi-coupled receptor, Glutathione peroxidase, GSTM4, Hdac, HDAC4, HLA-G, HOXA11, HSP, Hsp70, Hsp90, Hsp22/Hsp40/Hsp90, HSP90B1, HSPA1A/HSPA1B, HSPB6, INO80C, MHC Class II (complex), MLL, MLLT1, OPRM1, PDHA2, SLC16A1, SOD2, TFRC	1.00E-26
10	Cell death, cellular growth and proliferation, connective tissue development and function	BIRC3, CASP3, CASP7, Caspase, CCL2, CCL4, CD8, CDC6, CHEMOKINE, COX4I1, DFF, DFFA, DFFB, DR4/5, DUB, HERC6, Hsp27, IFIT5, Ifn gamma, IL-1R, IL1RN, Interferon alpha, LDL, MCL1, NAIP, NEDD4, PANX1, PDCD6IP, PLSCR3, RFFL, TNFRSF10B, TNFSF10, USP18, USP48, USP49	1.00E-26

The list of 852 target genes for the set of miRNAs downregulated in AD brains was uploaded into IPA. The top 10 functional networks showing a significant association with target genes are listed with rank, IPA functional network, molecules in the network, and p-value by the Fisher's Exact test. The molecular network entitled "Cell cycle, connective tissue development and function, cellular growth and proliferation" (Rank 4) is illustrated in Fig. 2.

target genes, such as TargetScan 5.1 (www.targetscan.org), PicTar (pictar.mdc-berlin.de), miRanda (www.microrna.org), MicroCosm (www.ebi.ac.uk/enright-srv/microcosm/htdocs/targets/v5), and Diana-microT 3.0 (diana.cslab.ece.ntua.gr/microT). However, the miRNA target prediction by these programs is often hampered by detection of numerous false positive targets. To avoid this problem, we explored the targets for AD-relevant 171 miRNAs of Wang's dataset by using the miRTarBase (mirtarbase.mbc.nctu.edu.tw), the recently established largest collection of more than 3500 manually curated miRNA-target interactions from 985 articles, all of which are experimentally validated by luciferase reporter assay, western blot, qRT-PCR, microarray experiments with overexpression or knockdown of miRNAs, or pulsed stable isotope labeling with amino acids in culture (pSILAC) experiments (Hsu et al., 2011) (Supplementary Tables 1 and 2).

Although experimentally validated targets represent a source of reliable candidates, it is worthless when they are not expressed in the human brain. Therefore, we verified the expression of target genes in the human brain at mRNA levels by analyzing them on UniGene (www.ncbi.nlm.nih.gov/unigene), an organized view of the transcriptome that semi-quantitatively exhibits the expression sequence tag (EST) profile as the number of transcripts per million (TPM). After omitting the genes undetectable in the human brain, we identified 852 non-redundant target genes for the set of miRNAs downregulated in AD brains (Supplementary Table 1). We also found 39 non-redundant target genes for the set of miRNAs upregulated in AD brains (Supplementary Table 2). Since the former greatly outnumbered the latter, thereafter, we have focused on molecular networks of 852 theoretically upregulated targets for the set of downregulated miRNAs in AD brains.

Next, we investigated molecular networks of 852 genes by searching them on the Database for Annotation, Visualization and Integrated Discovery (DAVID) (david.abcc.ncifcrf.gov), which automatically outputs the results from KEGG pathway analysis (Huang et al., 2009). When Entrez Gene IDs of 852 genes were imported into the
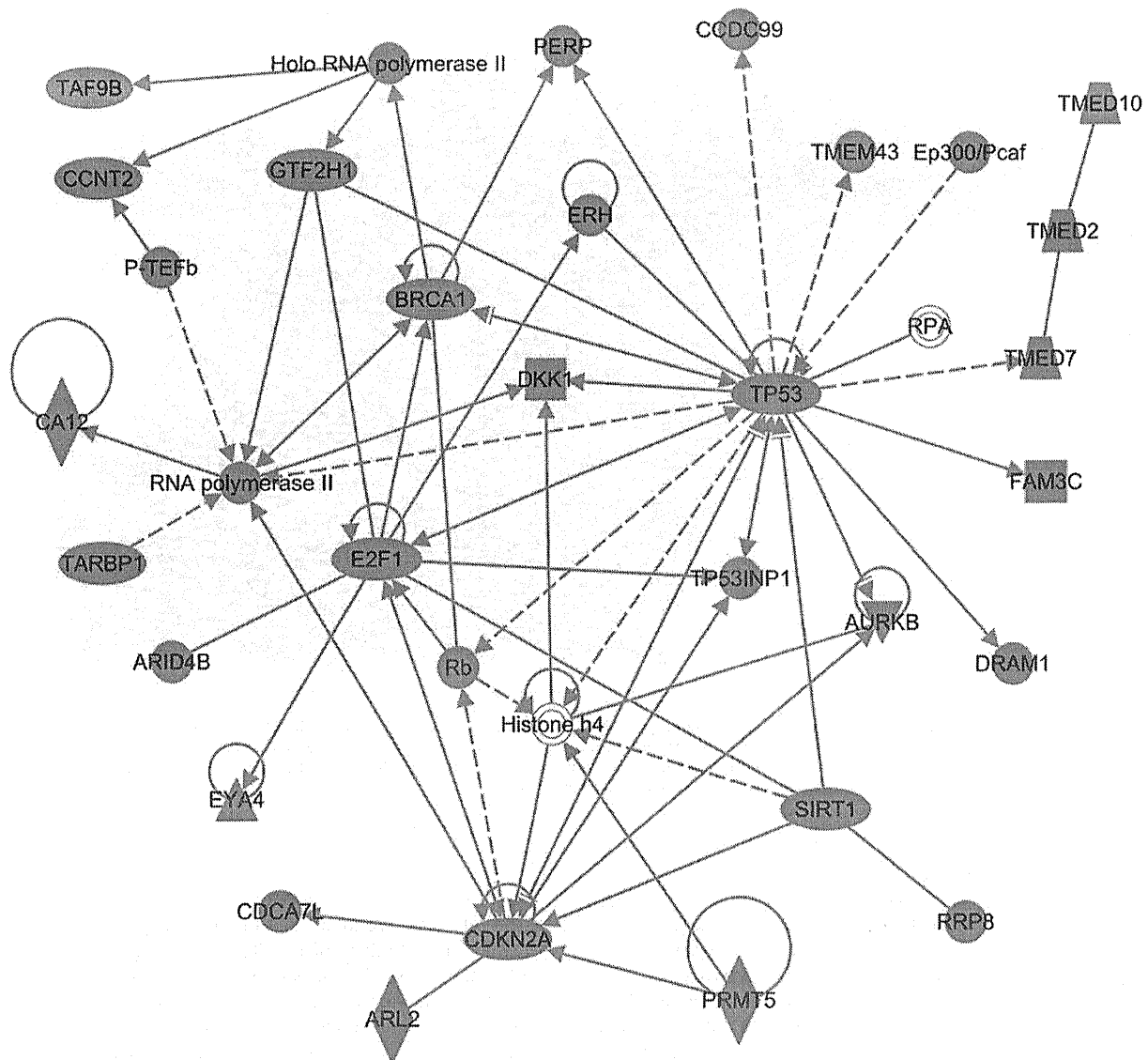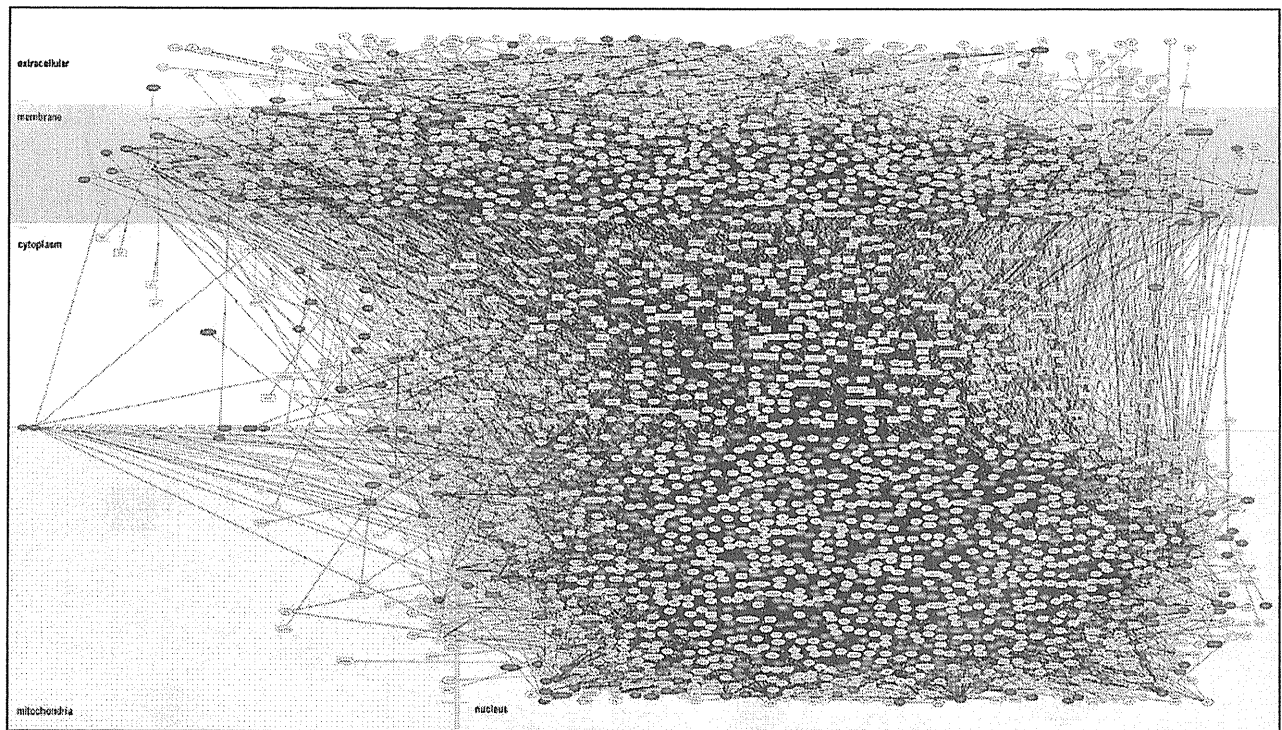
Fig. 2. Target genes for miRNAs downregulated in AD brains are located in the cell cycle-related network of IPA. The list of 852 target genes for the set of miRNAs downregulated in AD brains (Supplementary Table 1) was imported into IPA. Among the top 10 functional networks showing a significant association with target genes, the molecular network entitled "Cell cycle, connective tissue development and function, cellular growth and proliferation" (Rank 4 in Table 4) is illustrated. Target genes highlighted by red are potentially upregulated in AD brains.

Functional Annotation tool of DAVID, it identified a statistically significant association of the genes with several functional annotation categories (Table 2) and KEGG pathways (Table 3). The set of 852 genes showed a significant association with gene ontology (GO) terms related to regulation of cell proliferation, cell death, apoptosis, and cell cycle (Table 2). They also constructed KEGG pathways related to various types of cancers, cell cycle, focal adhesion, and signaling pathways of ErbB, p53, MAPK and TGF-beta (Table 3). Collectively, we concluded that a battery of cell cycle regulators, including cyclins, cyclin-dependent kinases (CDKs), cyclin-dependent kinase inhibitors (CDKIs), retinoblastoma protein (Rb), E2F family proteins, and p53, are highly enriched in both GO terms and KEGG pathways (Fig. 1).

Then, we validated the crucial involvement of cell cycle pathway in the molecular network of 852 target genes by uploading them into IPA and KeyMolnet. IPA suggested that these genes show a significant association with functional networks of cancer, cell growth, proliferation, development, and death, and cell cycle (Table 4). Again, major members of cell cycle regulators, including Rb, E2F1, and p53,

are clustered in these networks (Fig. 2). KeyMolnet, based on the neighboring network-search algorithm, extracted a highly complex network composed of 3428 molecules and 6837 molecular relations, exhibiting a significant association with transcriptional regulation by a battery of transcription factors, such as Rb/E2F, cAMP responsive element binding protein (CREB), glucocorticoid receptor (GR), vitamin D receptor (VDR), NF-κB, hypoxia inducible factor (HIF), p53, and AP-1 (Fig. 3) (Table 5). Although the molecular pathways and networks illustrated by three different programs KEGG, IPA, and KeyMolnet armed with distinct computational algorithms do not perfectly merge each other, all the results supported the working hypothesis that the set of miRNAs downregulated in AD brains induces abnormal regulation of cell cycle progression via synchronous upregulation of multiple cell cycle regulators.

The cell cycle progression is positively and negatively regulated by the complex checkpoint mechanism. Increasing evidence convincingly shows aberrant expression of cell cycle regulators in the hippocampus, the basal forebrain, and the cerebral cortex of AD brains. They

Fig. 3. KeyMolnet illustrates the highly complex molecular network of target genes for miRNAs downregulated in AD brains. The list of 852 target genes for the set of miRNAs downregulated in AD brains (Supplementary Table 1) was imported into KeyMolnet. The highly complex molecular network extracted by the neighboring network-search algorithm, composed of 3428 molecules and 6837 molecular relations, suggested the most significant relationship with the canonical pathway entitled "Transcriptional regulation by Rb/E2F" (Rank 1, Table 5). Target genes highlighted by red are potentially upregulated in AD brains.

include cyclins A, B, D, and E, along with CDKs and CDKIs of both the Cip/Kip and Ink4 families (Busser et al., 1998; McShea et al., 1997; Yang et al., 2003). The abnormal reentry into the cell cycle is an early event in neurons of AD brains stimulated by oxidative stress, which precedes Aβ deposition and NFT formation, and is potentially deleterious for terminally differentiated neurons, serving as a direct cause of neuronal apoptosis and degeneration (Bonda et al., 2010). The hypophosphorylated Rb protein interacts with the E2F family transcription factors E2F1, E2F2, and E2F3, and activates the expression of the genes pivotal for cell cycle progression, whereas the Rb protein, hyperphosphorylated by cyclin D1–CDK4 and cyclin E1–

Table 5
KeyMolnet pathways of target genes for miRNAs downregulated in AD brains.

Rank	KeyMolnet pathway	Score	Score p-value
1	Transcriptional regulation by Rb/E2F	882.46	2.25E-266
2	Transcriptional regulation by CREB	688.612	5.10E-208
3	Integrin family	630.668	1.41E-190
4	Transcriptional regulation by GR	508.344	9.40E-154
5	Transcriptional regulation by VDR	497.189	2.14E-150
6	Transcriptional regulation by NF-kB	495.71	5.98E-150
7	Transcriptional regulation by HIF	488.203	1.09E-147
8	TGF-beta family signaling pathway	387.147	2.87E-117
9	Transcriptional regulation by p53	386.348	4.98E-117
10	Transcriptional regulation by AP-1	367.719	2.02E-111

The list of 852 target genes for the set of miRNAs downregulated in AD brains was uploaded into KeyMolnet. It extracted a highly complex network composed of 3428 molecules and 6837 molecular relations, as illustrated in Fig. 3. The top 10 KeyMolnet pathways showing a significant association with target genes are listed with rank, KeyMolnet pathway, score, and p-value of the score. Abbreviations: Rb, retinoblastoma; CREB, cAMP responsive element binding protein; GR, glucocorticoid receptor; VDR, vitamin D receptor; NF-kB, nuclear factor kappa B; and HIF, hypoxia inducible factor.

CDK2 complexes, releases E2Fs, and represses the expression of cell cycle genes (Swiss and Casaccia, 2010). Thus, the Rb/E2F pathway constitutes a molecular switch deciding either progression or arrest of the cell cycle. We found that RB1 is an experimentally validated target for miR-23b, 26a, 106a, 106b, 124a and 335, while E2F1 is a target for miR-17, 20a, 21, 23b, 93, 98, 106a, 106b, 223 and 330, E2F2 for miR-21, 24 and 98, and E2F3 for miR-34a, 34c and 195 (Supplementary Table 3). Thus, it is evident that E2F1 serves as one of hub molecules that play a central role in the cell cycle pathway. All of these miRNAs are downregulated in AD brains in the dataset of Wang et al. (Table 1), suggesting the logical hypothesis that the levels of expression of Rb and E2F proteins are abnormally elevated in AD brains (Figs. 1 and 2). Most importantly, aberrant expression of Rb protein and E2F1 is actually identified in neurons and glia cells in the frontal cortex of AD brains, where the Rb protein is hyperphosphorylated (Ranganathan et al., 2001).

In conclusion, we identified 852 experimentally validated target genes for the set of miRNAs downregulated in AD brains by searching them on the miRTarBase and UniGene. The molecular network analysis of 852 target genes by using three distinct pathway analysis tools of bioinformatics KEGG, IPA, and KeyMolnet proposed the system biological view that aberrant expression of cell cycle regulators might serve as a direct cause of neurodegeneration in AD brains.

Supplementary materials related to this article can be found online at doi:10.1016/j.expneurol.2011.09.003.

References

Albert, R., Jeong, H., Barabasi, A.L., 2000. Error and attack tolerance of complex networks. Nature 406, 378–382.

Bettens, K., Brouwers, N., Engelborghs, S., Van Miegroet, H., De Deyn, P.P., Theuns, J., Sleegers, K., Van Broeckhoven, C., 2009. APP and BACE1 miRNA genetic variability has no major role in risk for Alzheimer disease. Hum. Mutat. 30, 1207–1213.

Boissonneault, V., Plante, I., Rivest, S., Provost, P., 2009. MicroRNA-298 and microRNA-328 regulate expression of mouse β-amyloid precursor protein-converting enzyme 1. J. Biol. Chem. 284, 1971–1981.

Bonda, D.J., Lee, H.P., Kudo, W., Zhu, X., Smith, M.A., Lee, H.G., 2010. Pathological implications of cell cycle re-entry in Alzheimer disease. Expert Rev. Mol. Med. 12, e19.

Busser, J., Geldmacher, D.S., Herrup, K., 1998. Ectopic cell cycle proteins predict the sites of neuronal cell death in Alzheimer's disease brain. J. Neurosci. 18, 2801–2807.

Cogswell, J.P., Ward, J., Taylor, I.A., Waters, M., Shi, Y., Cannon, B., Kelnar, K., Kemppainen, J., Brown, D., Chen, C., Prinjha, R.K., Richardson, J.C., Saunders, A.M., Roses, A.D., Richards, C.A., 2008. Identification of miRNA changes in Alzheimer's disease brain and CSF yields putative biomarkers and insights into disease pathways. J. Alzheimers Dis. 14, 27–41.

Cui, J.G., Li, Y.Y., Zhao, Y., Bhattacharjee, S., Lukiw, W.J., 2010. Differential regulation of interleukin-1 receptor-associated kinase-1 (IRAK-1) and IRAK-2 by microRNA-146a and NF-κB in stressed human astroglial cells and in Alzheimer disease. J. Biol. Chem. 285, 38951–38960.

Faghihi, M.A., Modarresi, F., Khalil, A.M., Wood, D.E., Sahagan, B.G., Morgan, T.E., Finch, C.E., St Laurent III, G., Kenny, P.J., Wahlestedt, C., 2008. Expression of a noncoding RNA is elevated in Alzheimer's disease and drives rapid feed-forward regulation of β-secretase. Nat. Med. 14, 723–730.

Faghihi, M.A., Zhang, M., Huang, J., Modarresi, F., Van der Brug, M.P., Nalls, M.A., Cookson, M.R., St-Laurent III, G., Wahlestedt, C., 2010. Evidence for natural antisense transcript-mediated inhibition of microRNA function. Genome Biol. 11, R56.

Filipowicz, W., Bhattacharyya, S.N., Sonenberg, N., 2008. Mechanisms of post-transcriptional regulation by microRNAs: are the answers in sight? Nat. Rev. Genet. 9, 102–114.

Fineberg, S.K., Kosik, K.S., Davidson, B.L., 2009. MicroRNAs potentiate neural development. Neuron 64, 303–309.

Friedman, R.C., Farh, K.K., Burge, C.B., Bartel, D.P., 2009. Most mammalian mRNAs are conserved targets of microRNAs. Genome Res. 19, 92–105.

Harraz, M.M., Dawson, T.M., Dawson, V.L., in press. MicroRNAs in Parkinson's disease. J. Chem. Neuroanat.

Hébert, S.S., Horré, K., Nicolaï, L., Papadopoulou, A.S., Mandemakers, W., Silahtaroglu, A.N., Kauppinen, S., Delacourte, A., De Strooper, B., 2008. Loss of microRNA cluster miR-29a/b-1 in sporadic Alzheimer's disease correlates with increased BACE1/beta-secretase expression. Proc. Natl. Acad. Sci. U. S. A. 105, 6415–6420.

Hébert, S.S., Horré, K., Nicolaï, L., Bergmans, B., Papadopoulou, A.S., Delacourte, A., De Strooper, B., 2009. MicroRNA regulation of Alzheimer's amyloid precursor protein expression. Neurobiol. Dis. 33, 422–428.

Hébert, S.S., Papadopoulou, A.S., Smith, P., Galas, M.C., Planel, E., Silahtaroglu, A.N., Sergeant, N., Buée, L., De Strooper, B., 2010. Genetic ablation of Dicer in adult forebrain neurons results in abnormal tau hyperphosphorylation and neurodegeneration. Hum. Mol. Genet. 19, 3959–3969.

Hsu, C.W., Juan, H.F., Huang, H.C., 2008. Characterization of microRNA-regulated protein-protein interaction network. Proteomics 8, 1975–1979.

Hsu, S.D., Lin, F.M., Wu, W.Y., Liang, C., Huang, W.C., Chan, W.L., Tsai, W.T., Chen, G.Z., Lee, C.J., Chiu, C.M., Chien, C.H., Wu, M.C., Huang, C.Y., Tsou, A.P., Huang, H.D., 2011. miRTarBase: a database curates experimentally validated microRNA-target interactions. Nucleic Acids Res. 39, D163–D169.

Huang, da W., Sherman, B.T., Lempicki, R.A., 2009. Systematic and integrative analysis of large gene lists using DAVID bioinformatics resources. Nat. Protoc. 4, 44–57.

Kanehisa, M., Goto, S., Furumichi, M., Tanabe, M., Hirakawa, M., 2010. KEGG for representation and analysis of molecular networks involving diseases and drugs. Nucleic Acids Res. 38, D355–D360.

Kitano, H., 2007. A robustness-based approach to systems-oriented drug design. Nat. Rev. Drug Discov. 6, 202–210.

Kocerha, J., Kauppinen, S., Wahlestedt, C., 2009. microRNAs in CNS disorders. Neuromolecular Med. 11, 162–172.

Lukiw, W.J., 2007. Micro-RNA speciation in fetal, adult and Alzheimer's disease hippocampus. Neuroreport 18, 297–300.

Lukiw, W.J., Zhao, Y., Cui, J.G., 2008. An NF-κB-sensitive micro RNA-146a-mediated inflammatory circuit in Alzheimer disease and in stressed human brain cells. J. Biol. Chem. 283, 31315–31322.

Maes, T., Barceló, A., Buesa, C., 2002. Neuron navigator: a human gene family with homology to unc-53, a cell guidance gene from *Caenorhabditis elegans*. Genomics 80, 21–30.

Maes, O.C., Chertkow, H.M., Wang, E., Schipper, H.M., 2009. MicroRNA: implications for Alzheimer disease and other human CNS disorders. Curr. Genomics 10, 154–168.

McShea, A., Harris, P.L., Webster, K.R., Wahl, A.F., Smith, M.A., 1997. Abnormal expression of the cell cycle regulators P16 and CDK4 in Alzheimer's disease. Am. J. Pathol. 150, 1933–1939.

Mitchell, P.S., Parkin, R.K., Kroh, E.M., Fritz, B.R., Wyman, S.K., Pogosova-Agadjanyan, E.L., Peterson, A., Noteboom, J., O'Briant, K.C., Allen, A., Lin, D.W., Urban, N., Drescher, C.W., Knudsen, B.S., Stirewalt, D.L., Gentleman, R., Vessella, R.L., Nelson, P.S., Martin, D.B., Tewari, M., 2008. Circulating microRNAs as stable blood-based markers for cancer detection. Proc. Natl. Acad. Sci. U. S. A. 105, 10513–10518.

Nelson, P.T., Wang, W.X., 2010. MiR-107 is reduced in Alzheimer's disease brain neocortex: validation study. J. Alzheimers Dis. 21, 75–79.

Nelson, P.T., Wang, W.X., Rajeev, B.W., 2008. MicroRNAs (miRNAs) in neurodegenerative diseases. Brain Pathol. 18, 130–138.

Nelson, P.T., Dimayuga, J., Wilfred, B.R., 2010. MicroRNA in situ hybridization in the human entorhinal and transentorhinal cortex. Front. Hum. Neurosci. 4, 7.

Nunez-Iglesias, J., Liu, C.C., Morgan, T.E., Finch, C.E., Zhou, X.J., 2010. Joint genome-wide profiling of miRNA and mRNA expression in Alzheimer's disease cortex reveals altered miRNA regulation. PLoS One 5, e8898.

Ranganathan, S., Scudiere, S., Bowser, R., 2001. Hyperphosphorylation of the retinoblastoma gene product and altered subcellular distribution of E2F-1 during Alzheimer's disease and amyotrophic lateral sclerosis. J. Alzheimers Dis. 3, 377–385.

Satoh, J., 2010. MicroRNAs and their therapeutic potential for human diseases: aberrant microRNA expression in Alzheimer's disease brains. J. Pharmacol. Sci. 114, 269–275.

Satoh, J., Tabunoki, H., 2011. Comprehensive analysis of human microRNA target networks. BioData Min. 4, 17.

Satoh, J., Tabunoki, H., Arima, K., 2009. Molecular network analysis suggests aberrant CREB-mediated gene regulation in the Alzheimer disease hippocampus. Dis. Markers 27, 239–252.

Schratt, G.M., Tuebing, F., Nigh, E.A., Kane, C.G., Sabatini, M.E., Kiebler, M., Greenberg, M.E., 2006. A brain-specific microRNA regulates dendritic spine development. Nature 439, 283–289.

Selbach, M., Schwanhäusser, B., Thierfelder, N., Fang, Z., Khanin, R., Rajewsky, N., 2008. Widespread changes in protein synthesis induced by microRNAs. Nature 455, 58–63.

Sethi, P., Lukiw, W.J., 2009. Micro-RNA abundance and stability in human brain: specific alterations in Alzheimer's disease temporal lobe neocortex. Neurosci. Lett. 459, 100–104.

Shioya, M., Obayashi, S., Tabunoki, H., Arima, K., Saito, Y., Ishida, T., Satoh, J., 2010. Aberrant microRNA expression in the brains of neurodegenerative diseases: miR-29a decreased in Alzheimer disease brains targets neuron navigator-3. Neuropathol. Appl. Neurobiol. 36, 320–330.

Smith, P., Al Hashimi, A., Girard, J., Delay, C., Hébert, S.S., 2011. In vivo regulation of amyloid precursor protein neuronal splicing by microRNAs. J. Neurochem. 116, 240–247.

Swiss, V.A., Casaccia, P., 2010. Cell-context specific role of the E2F/Rb pathway in development and disease. Glia 58, 377–390.

Vasudevan, S., Tong, Y., Steitz, J.A., 2007. Switching from repression to activation: microRNAs can up-regulate translation. Science 318, 1931–1934.

Vilardo, E., Barbato, C., Ciotti, M., Cogoni, C., Ruberti, F., 2010. MicroRNA-101 regulates amyloid precursor protein expression in hippocampal neurons. J. Biol. Chem. 285, 18344–18351.

Viswanathan, G.A., Seto, J., Patil, S., Nudelman, G., Sealfon, S.C., 2008. Getting started in biological pathway construction and analysis. PLoS Comput. Biol. 4, e16.

Wang, W.X., Rajeev, B.W., Stromberg, A.J., Ren, N., Tang, G., Huang, Q., Rigoutsos, I., Nelson, P.T., 2008. The expression of microRNA miR-107 decreases early in Alzheimer's disease and may accelerate disease progression through regulation of β-site amyloid precursor protein-cleaving enzyme 1. J. Neurosci. 28, 1213–1223.

Wang, W.X., Huang, Q., Hu, Y., Stromberg, A.J., Nelson, P.T., 2011. Patterns of microRNA expression in normal and early Alzheimer's disease human temporal cortex: white matter versus gray matter. Acta Neuropathol. 121, 193–205.

Yang, Y., Mufson, E.J., Herrup, K., 2003. Neuronal cell death is preceded by cell cycle events at all stages of Alzheimer's disease. J. Neurosci. 23, 2557–2563.

Yao, J., Hennessey, T., Flynt, A., Lai, E., Beal, M.F., Lin, M.T., 2010. MicroRNA-related cofilin abnormality in Alzheimer's disease. PLoS One 5, e15546.

SHORT COMMUNICATION

Gene Expression Profile of THP-1 Monocytes Following Knockdown of DAP12, A Causative Gene for Nasu-Hakola Disease

Jun-ichi Satoh · Yoshihiro Shimamura · Hiroko Tabunoki

Abstract Nasu-Hakola disease (NHD), also designated polycystic lipomembranous osteodysplasia with sclerosing leukoencephalopathy, is a rare autosomal recessive disorder characterized by progressive presenile dementia and formation of multifocal bone cysts, caused by a loss-of-function mutation of DAP12 or TREM2. TREM2 and DAP12 constitute a receptor/adaptor complex expressed on osteoclasts, dendritic cells, macrophages, monocytes, and microglia. At present, the precise molecular mechanisms underlying development of leukoencephalopathy and bone cysts in NHD remain largely unknown. We established THP-1 human monocyte clones that stably express small interfering RNA targeting DAP12 for serving as a cellular model of NHD. Genome-wide transcriptome analysis identified a set of 22 genes consistently downregulated in DAP12 knockdown cells. They constituted the molecular network closely related to the network defined by cell-to-cell signaling and interaction, hematological system development and function, and inflammatory response, where NF-κB acts as a central regulator. These results suggest that a molecular defect of DAP12 in human monocytes deregulates the gene network pivotal for maintenance of myeloid cell function in NHD.

Keywords DAP12 · IPA · Knockdown · Nasu-Hakola disease · Microarray · THP-1

List of Abbreviations
ALX1   ALX homeobox 1

DAP12   DNAX-activation protein 12
IBA1   Ionized calcium-binding adapter molecule 1
IPA   Ingenuity pathways analysis
NAV3   Neuron navigator 3
NHD   Nasu-Hakola disease
PLOSL   Polycystic lipomembranous osteodysplasia with sclerosing leukoencephalopathy
siRNA   Small interfering RNA
TREM2   Triggering receptor expressed on myeloid cells 2
TYROBP   TYRO protein tyrosine kinase-binding protein

Introduction

Nasu-Hakola disease (NHD; OMIM 221770), also designated polycystic lipomembranous osteodysplasia with sclerosing leukoencephalopathy (PLOSL), is a rare autosomal recessive disorder, characterized by progressive presenile dementia and formation of multifocal bone cysts (Bianchin et al. 2004). Typically, the patients show pathological bone fractures during the third decade of life, and a frontal lobe syndrome during the fourth decade of life, followed by death by age 50 years due to profound dementia and loss of mobility. The neuropathological hallmark includes extensive demyelination, accumulation of axonal spheroids, and intense astrogliosis predominantly in the frontal and temporal lobes and the basal ganglia (Tanaka 2000).

NHD is caused by a homozygous mutation located in one of the two genes, DNAX-activation protein 12 (DAP12), alternatively named TYRO protein tyrosine kinase-binding protein (TYROBP) on chromosome 19q13.1 or triggering receptor expressed on myeloid cells 2 (TREM2) on chromosome 6p21.1 (Klünemann et al. 2005). Currently, 17

J. Satoh (✉) · Y. Shimamura · H. Tabunoki
Department of Bioinformatics and Molecular Neuropathology,
Meiji Pharmaceutical University, 2-522-1 Noshio, Kiyose,
Tokyo 204-8588, Japan
e-mail: satoj@my-pharm.ac.jp

🍃 Springer

different loss-of-function mutations are identified in either DAP12 or TREM2, all of which cause an identical disease phenotype. TREM2 and DAP12 constitute a receptor/adaptor complex expressed on myeloid cells, such as osteoclasts, dendritic cells, monocytes/macrophages, and microglia, although the genuine ligand for TREM2 has not yet been identified (Turnbull and Colonna 2007). Previously, several lines of DAP12-deficient/loss-of-function mice have been established by using different targeting strategies (Kaifu et al. 2003; Roumier et al. 2004; Nataf et al. 2005; Otero et al. 2009). However, none of these mice exhibited multifocal bone cysts and sclerosing leukoencephalopathy, the essential phenotype of NHD. At present, the precise molecular mechanisms responsible for brain and bone lesion development in NHD remain largely unknown, in part owing to a lack of adequate human cellular models.

In this study, we established clonal THP-1 human monocytes that stably express small interfering RNA (siRNA) targeting DAP12 for serving as a cellular model for studying NHD. By genome-wide transcriptome analysis, we identified a set of genes consistently downregulated in DAP12 knockdown cells. Our results suggest that a molecular defect of DAP12 in human monocytes deregulates the gene network pivotal for maintenance of myeloid cell function in NHD.

Methods

Human Monocyte Cell Line

The human cell line THP-1 originated from acute monocytic leukemia was provided by Riken Cell Bank, Tsukuba, Ibaraki, Japan. The cells were maintained in RPMI 1640 medium (Invitrogen, Carlsbad, CA, USA) supplemented with 10% fetal bovine serum (FBS), 55 µM 2-mercaptoethanol, 2 mM L-glutamine, 100 U/ml penicillin, and 100 µg/ml streptomycin (feeding medium).

Vector Construction

The siRNA vector construct targeting the DAP12 sequence (SI) and the control vector construct targeting the scrambled sequence (SCR) were generated by using GeneClip U1 Hairpin cloning system (Promega, Madison, WI, USA). The following sense and antisense oligonucleotides are utilized: 5′ tctcgtcagaggtcggatgtctacttcctgtcatagacatccgacctctgacct 3′ and 5′ ctgcaggtcagaggtcggatgtctatgacaggaagtagacatccgacctc tgac 3′ for generation of SI and 5′ tctcgacgtctgtgcgaagttgact tcctgtcatcaacttcgcacagacgtcct 3′ and 5′ ctgcaggacgtctgtgcga agttgatgacaggaagtcaacttcgcacagacgtc 3′ for generation of SCR.

Isolation of THP-1 Clones Stably Expressing siRNA Targeting DAP12

The vectors were linearized and transfected in THP-1 cells by using Lipofectamine LTX reagent (Invitrogen). The stable cell lines were selected by incubating them for ∼2 months in the feeding medium with inclusion of 200 µg/ml Hygromycin B (Invitrogen). Then, four distinct stable clones were selected by limiting dilution of the cells in a manner of a single cell per well plated in a 96-well cell culture plate. In some experiments, the cells were incubated for 24 h in the feeding medium containing 50 nM phorbol 12-myristate 13-acetate (PMA) (Sigma, St. Louis, MO, USA) or vehicle (dimethyl sulfoxide; DMSO). Incorporation of the transgenes was validated by RT-PCR using the primer set composed of 5′ gaagtgagaatcccagctgtgtg 3′ and 5′ gccgcccagtctactttttgaaact 3′ derived from the vector sequences surrounding the insert.

Western Blot Analysis

To prepare total protein extract, the cells were homogenized in RIPA buffer supplemented with a cocktail of protease inhibitors (Sigma). The protein extract was centrifuged at 12,000 rpm for 5 min at room temperature (RT). The concentration of protein was determined by a Bradford assay kit (BioRad Hercules, CA, USA). The mixture of the supernatant and a 2× Lammeli loading buffer was boiled, and separated on a 12% SDS-PAGE gel. After gel electrophoresis, the protein was transferred onto nitrocellulose membranes, and immunolabeled at RT overnight with rabbit anti-DAP12 antibody (sc-20783; Santa Cruz Biotechnology, Santa Cruz, CA). Then, the membranes were incubated at RT for 60 min with HRP-conjugated anti-rabbit IgG (Santa Cruz Biotechnology). The specific reaction was visualized by exposing the membranes to a chemiluminescent substrate (Thermo Scientific, Rockford, IL, USA). Then, the antibodies were stripped by incubating the membranes at 50°C for 30 min in stripping buffer, composed of 62.5 mM Tris–HCl, pH 6.7, 2% SDS, and 100 mM 2-mercaptoethanol. The membranes were processed for relabeling with goat anti-heat shock protein HSP60 antibody (sc-1052, N-20; Santa Cruz Biotechnology) for an internal control of protein loading, followed by incubation with HRP-conjugated anti-goat IgG.

Microarray Analysis

Total cellular RNA was isolated by using the TRIZOL Plus RNA Purification kit (Invitrogen). The quality of total RNA was evaluated on Agilent 2100 Bioanalyzer (Agilent Technologies, Palo Alto, CA, USA). 300 ng of total RNA

was processed for cRNA synthesis, fragmentation, and terminal labeling with the GeneChip Whole Transcript Sense Target Labeling and Control Reagents (Affymetrix, Santa Clara, CA, USA). Then, it was processed for hybridization at 45°C for 17 h with Human Gene 1.0 ST Array that contains 28,869 genes (Affymetrix). The arrays were washed in the GeneChip Fluidic Station 450 (Affymetrix), and scanned by the GeneChip Scanner 3000 7G (Affymetrix). The raw data, expressed as CEL files, were normalized by the robust multiarray average (RMA) method with the Expression Console software version 1.1 (Affymetrix).

Quantitative RT-PCR Analysis

Total cellular RNA was treated with DNase I, and was processed for cDNA synthesis using oligo(dT)$_{20}$ primers and SuperScript II reverse transcriptase (Invitrogen). cDNA was amplified by PCR in LightCycler ST300 (Roche Diagnostics, Tokyo, Japan) using SYBR Green I and following sense and antisense primer sets: 5′ tcggatgtctacagcgacctcaac 3′ and 5′ tcgcggtaggagttggaatgaggt 3′ for an 135 bp product of DAP12; 5′ ggtcttccagtatcgcagttcttc 3′ and 5′ ccacacacagca gcttattgtggt 3′ for an 164 bp product of ALX homeobox 1 (ALX1); 5′ tgacccagagttgtggtctccaag 3′ and 5′ gtccagtttgg ctatcccatgtgc 3′ for a 203 bp product of neuron navigator 3 (NAV3); and 5′ ccatgttcgtcatgggtgtgaacca 3′ and 5′ gccagt agaggcagggatgatgttc 3′ for a 251 bp product of the glyceraldehyde-3-phosphate dehydrogenase (G3PDH) gene. The expression levels of target genes were standardized against the levels of G3PDH, an internal control, detected in corresponding cDNA samples. All the assays were performed in triplicate.

In some experiments, cDNA was amplified by the conventional PCR using HotStar Taq DNA polymerase (Qiagen, Valencia, CA, USA) and following sense and antisense primer sets: 5′ agtgaggctgacaccctcaggaa 3′ and 5′ agat gctgtgctccacatggca 3′ for an 133 bp product of TREM2; 5′ cagggttccggtgttcaacattgt 3′ and 5′ ttggcacaactgccagatgg atgt 3′ for an 171 bp product of TREM1; and 5′ catgtccctg aaacgaatgctgga 3′ and 5′ atctcttgcccagcatcatcctga 3′ for an 143 bp product of ionized calcium-binding adapter molecule 1 (IBA1), a cell type-specific marker of macrophages/microglia.

Molecular Network Analysis

Ingenuity pathways analysis (IPA) is a knowledgebase that contains ~2,500,000 biological and chemical interactions and functional annotations with scientific evidence. They are collected from more than 500 selected articles, textbooks and other data sources, manually curated by expert biologists. By uploading the gene list, the network-generation algorithm identifies focused genes integrated in a global molecular network. IPA calculates the score P value, the statistical significance of association between the genes and the network evaluated by the Fisher's exact test.

Results

### Establishment of THP-1 Clones Expressing siRNA Targeting DAP12

First of all, by RT-PCR, we identified the expression of DAP12, TREM2, TREM1, and IBA1 in the human monocyte cell line THP-1, as well as in peripheral blood mononuclear cells (PBMC) (Fig. 1a–d, lanes 1, 2). These results suggest that THP-1 cells serve as a cellular model useful for studying biological functions of the TREM2/DAP12 receptor/adaptor complex. Then, the SI vector targeting DAP12 or the SCR vector expressing the scrambled sequence was transfected in THP-1 cells, and clonal cells stably expressing transgenes were selected by limiting dilution. We established two SI clones named SI5 and SI17, in addition to two SCR clones named SCR1 and SCR4. By RT-PCR, we verified the expression of transgenes in all of these clones (Fig. 1f, lanes 1–4). Western blot analysis showed that the levels of DAP12 protein expression were greatly reduced in SI5 and SI17 clones (Fig. 1h, lanes 1, 2).

Gene Expression Profile of DAP12 Knockdown THP-1 Clones

To identify the genes deregulated in THP-1 clones by DAP12 knockdown, potentially relevant to loss-of-function of DAP12 in NHD, we studied the genome-wide transcriptome on a microarray. In two separate sets of the experiments, we identified a set of 22 genes downregulated reproducibly by greater than a 50% reduction in SI17 versus SCR4 cells (Table 1). They include TYROBP (DAP12), supporting the validity of the experiments. Quantitative RT-PCR validated downregulation of ALX1, NAV3, and DAP12 in SI5 and SI17 cells, compared with the levels in SCR1 and SCR4 cells (Fig. 2a–f). Since, both SI5 and SI17 cells are established as independent clones, these observations excluded the possibility of non-specific gene silencing effects mediated by random incorporation of transgenes in the genome. Furthermore, we found that SI17 and SCR4 cells were capable of equally responding to PMA, a known inducer of morphological differentiation of THP-1 cells, by exhibiting almost similar gene expression profiles between both, following exposure to PMA (data not shown).

Fig. 1 Establishment of DAP12 knockdown THP-1 Clones. **a** DAP12, **b** TREM2, **c** TREM1, **d** IBA1, and **e** G3PDH mRNA expression in THP-1 (*lane 1*) and peripheral blood mononuclear cells (PBMC) (*lane 2*) determined by RT-PCR. The 100-bp ladder marker is shown on the *left*. **f** Indicates transgene and **g** G3PDH (an internal control) mRNA expression determined by RT-PCR, and **h** DAP12 and **i** HSP60 (an internal control) protein expression determined by western blot. *Lane 1* SI5 siRNA-expressing clone, *lane 2* SI17 siRNA-expressing clone, *lane 3* SCR1 scramble RNA-expressing clone, *lane 4* SCR4 scramble RNA-expressing clone, and *lane 5* wild-type (WT) THP-1 cells
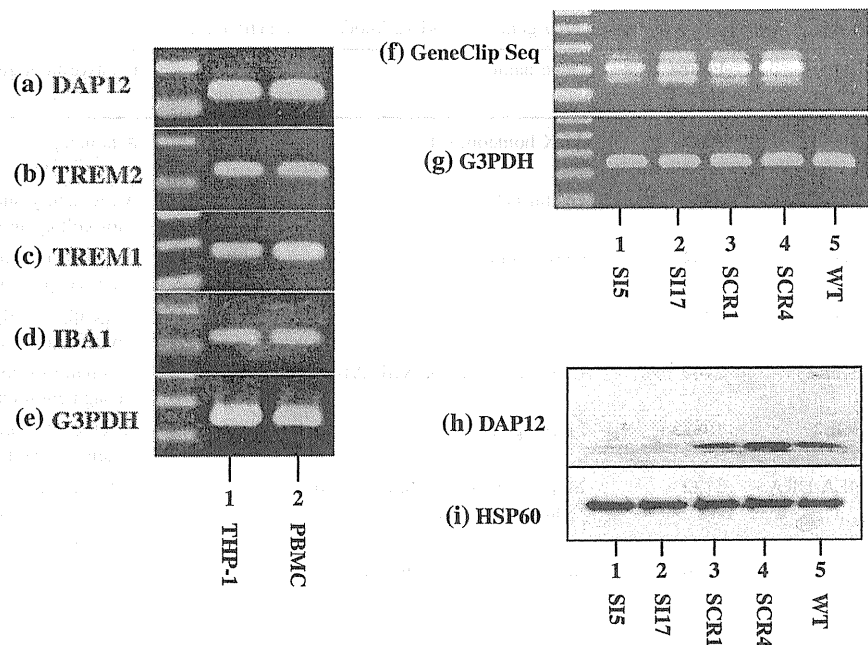
Finally, we imported the set of 22 genes into IPA, a tool for analyzing molecular network on the comprehensive knowledgebase. IPA illustrated a molecular network showing the most significant relationship with the network defined by "cell-to-cell signaling and interaction, hematological system development and function, and inflammatory response" ($P = 1 \times 10\text{E-}29$) (Fig. 2g). In this network, the nuclear factor-kappa B (NF-κB) complex acts as a central regulator for the set of downregulated genes in DAP12 knockdown cells. Recently, by microarray analysis, we identified 188 downregulated genes, composed of various GABA receptor subunits and synaptic components, in the brain of a NHD patient with a splicing mutation of TREM2 (Numasawa et al. 2011). Although, there exists no overlap between the set of 188 genes downregulated in the NHD brain and the set of 22 genes downregulated in DAP12 knockdown THP-1 cells, the molecular network of 188 genes showed the most significant relationship with the network defined by "neurological disease, organismal injury and abnormalities, and behavior" ($P = 1 \times 10\text{E-}66$), where NF-$\kappa$B again acts as a key regulator (Fig. 2h).

Discussion

NHD is caused by genetic mutations of DAP12 or TREM2 (Klünemann et al. 2005). However, at present, the precise molecular mechanism responsible for development of multiple bone cysts and sclerosis encephalopathy in NHD remains largely unknown, in part due to the lack of an adequate human cellular model. Previous studies showed

that DAP12-deficient mice are affected with osteopetrosis, hypomyelinosis, and synaptic degeneration, suggesting that DAP12 signaling is pivotal for development of osteoclasts and oligodendrocytes, and synaptogenesis (Kaifu et al. 2003; Roumier et al. 2004). Furthermore, the number of microglia is substantially reduced in the brain of DAP12-deficient/loss-of-function mice (Nataf et al. 2005; Otero et al. 2009). However, none of these mice exhibited multifocal bone cysts and sclerosing leukoencephalopathy, the most essential phenotype of NHD. By immunohistochemistry, we recently found that TREM2 is not expressed constitutively on human microglia, and DAP12-deficient Iba1-positive microglia are well preserved in the brains of NHD patients with DAP12 mutations (Satoh et al. 2011). Thus, DAP12-knockout mouse models have not fully replicated the phenotype of the human disease.

To obtain a cellular model for studying NHD, we have established THP-1 human monocyte clones stably expressing siRNA targeting DAP12 (SI) or scrambled RNA (SCR). The genome-wide transcriptome analysis identified a set of 22 genes downregulated by DAP12 knockdown, which constituted the molecular network of cell-to-cell signaling and interaction, hematological system development and function, and inflammatory response, where NF-κB acts as a central regulator. Importantly, the pivotal role of NF-κB was verified in the molecular network of the genes downregulated in the brain of a NHD patient.

The trimolecular complex composed of TREM2 monomer and DAP12 homodimer constitute a receptor/adaptor complex expressed on myeloid cells, such as osteoclasts,

Table 1 Twenty-two downregulated genes in DAP12 knockdown THP-1 cells

Gene symbol	Entrez gene ID	Gene name	Putative biological function
ALX1	8092	ALX homeobox 1	A homeoprotein necessary for survival of the forebrain mesenchyme
CCND2	894	Cyclin D2	A regulatory subunit of CDK4 or CDK6 required for cell cycle G1/S transition
CD180	4064	CD180 molecule	A cell surface molecule of the TLR family that forms the receptor complex with MD-1
CD4	920	CD4 molecule	A membrane glycoprotein of T lymphocytes that interacts with major histocompatibility complex class II antigens
F13A1	2162	Coagulation factor XIII, A1 polypeptide	A subunit of coagulation factor XIII activated in the blood coagulation cascade
FGL2	10875	Fibrinogen-like 2	A secreted protein of lymphocytes similar to the beta- and gamma-chains of fibrinogen
HLA-DRA	3122	Major histocompatibility complex, class II, DR alpha	A HLA class II alpha chain paralogue that plays a central role in presenting peptides derived from extracellular proteins
IFI16	3428	Interferon, gamma-inducible protein 16	An IFN-gamma-inducible protein involved in antiviral defense, regulation of cell growth and differentiation, and modulation of immune function
NAV3	89795	Neuron navigator 3	A protein of the neuron navigator family predominantly expressed in the central and peripheral nervous system
ORM1	5004	Orosomucoid 1	An acute phase plasma protein that acts as an immunomodulator
OVOS	408186	Ovostatin	A proteinase inhibitor with a strong anti-collagenase activity
SERPINF1	5176	Serpin peptidase inhibitor, clade F (alpha-2 antiplasmin, pigment epithelium derived factor), member 1	A secreted protein of the serpin family involved in inhibition of angiogenesis
SLC7A2	6542	Solute carrier family 7 (cationic amino acid transporter, y + system), member 2	A cationic amino acid transporter
SLC8A1	6546	Solute carrier family 8 (sodium/calcium exchanger), member 1	A Na(+)–Ca(2+) exchanger abundantly expressed in the heart and the brain
TMEM116	89894	Transmembrane protein 116	A transmembrane protein of unknown function
TRIM22	10346	Tripartite motif-containing 22	A member of the TRIM family induced by interferon involved in antiviral defense
TYROBP	7305	TYRO protein tyrosine kinase-binding protein	A transmembrane signaling protein containing an ITAM expressed on myeloid cells
VAT1L	57687	Vesicle amine transport protein 1 homolog (*Torpedo californica*)-like	A vesicle amine transport protein 1 homolog
ZNF426	79088	Zinc finger protein 426	A suppressor of RTA-mediated Kaposi's sarcoma-associated herpesvirus reactivation
ZNF506	440515	Zinc finger protein 506	A PML-associated repressor of transcription
ZNF717	100131827	Zinc finger protein 717	A zinc finger protein of unknown function
ZNF788	388507	Zinc finger family member 788	A zinc finger protein of unknown function

The transcriptome of THP-1 clones stably expressing DAP12 siRNA (SI17) and scrambled RNA (SCR4) on human gene 1.0 ST array are compared. In two separate sets of the experiments, the genes consistently downregulated by greater than a 50% reduction in SI17 versus SCR4 are listed in an alphabetical order

dendritic cells, monocytes/macrophages, and microglia (Turnbull and Colonna 2007). DAP12 also serves as an adaptor for TREM1, NCR2 (NKp44), SIRPB1, and MDL1. Following stimulation of the receptors, these complexes transmit signals via rapid phosphorylation of the immunoreceptor tyrosine-based activating motif (ITAM) of DAP12 mediated by Src protein tyrosine kinases (PTKs). Then, phosphorylated ITAM provides a docking site for the Src homology 2 (SH2) domains of spleen tyrosine kinase (Syk). Recruitment of Syk to phosphorylated ITAM transduces downstream signals through activation of phosphatidylinositol-3 kinase (PI3K), phospholipase C (PLC), protein
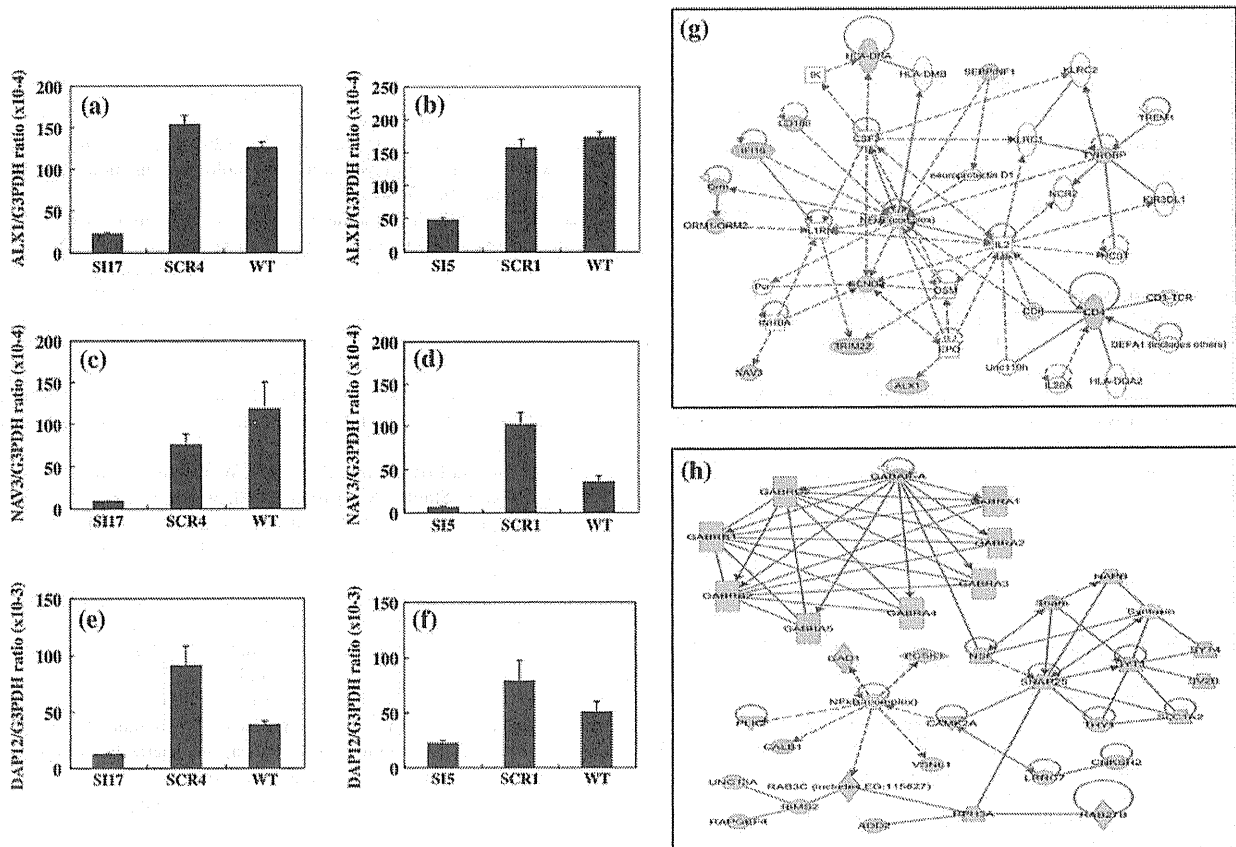
Fig. 2 Gene expression profiles of DAP12 knockdown THP-1 clones. a, b ALX1, c, d NAV3, and e, f DAP12 mRNA expression in SI17, SCR4, and WT cells (a, c, e) and SI5, SCR1, and WT cells (b, d, f) determined by quantitative RT-PCR. The expression levels of target genes are standardized against the levels of G3PDH. g, h Molecular networks determined by IPA of g the set of 22 genes downregulated in DAP12 knockdown THP-1 cells (Table 1) and h the set of 188 genes downregulated in the brain of a NHD patient

(Numasawa et al. 2011). The network g showed the most significant relationship with the network defined by "cell-to-cell signaling and interaction, hematological system development and function, and inflammatory response", while the network h exhibited the most significant relationship with the network defined by "neurological disease, organismal injury, and abnormalities, and behavior". In both of these networks, the transcription factor nuclear factor-kappa B (NF-κB) complex acts as a key regulator

kinase C (PKC), and mitogen-activated protein kinase (MAPK) (Mócsai et al. 2010). Furthermore, Syk activation induces tyrosine phosphorylation of RelA (p65), a central component of the canonical pathway of NF-κB, resulting in enhancement of its transcriptional activity (Bijli et al. 2008). Thus, DAP12 signaling pathway has a close link with the NF-κB pathway, a principal regulator of immune function.

Although, previous studies showed that TREM2 binds to polyanionic macromolecules, bacteria, heat shock proteins, and apoptotic neuronal cell membranes (Stefano et al. 2009), the functional ligand has not yet been characterized. Both DAP12 knockdown and control THP-1 monocyte clones we established might express TREM2 (Fig. 1b) and help us to perform in vitro high-throughput screening of endogenous TREM2 ligands.

Among the set of downregulated genes by DAP12 knockdown, ALX1 is a paired-type homeoprotein that

plays an important role in craniofacial bone formation and limb development. A homozygous deletion of the ALX gene causes severe microphthalmia and facial clefting (Uz et al. 2010). CD180, also designated RP105, is a cell surface molecule of the Toll-like receptor (TLR) family expressed on B cells and monocytes, which forms the receptor complex with MD-1. The RP105/MD-1 complex acts as a negative regulator of TLR4/MD-2 signaling (Divanovic et al. 2007). Importantly, TREM2 inhibits cytokine production by macrophages in response to the TLR4 ligand lipopolysaccharide (LPS) (Turnbull et al. 2006). NAV3 is a member of the neuron navigator protein family expressed predominantly in the central and peripheral nervous systems. In adult mouse brain, NAV3 is expressed chiefly in nuclear membranes of neurons in the cerebral cortex, midbrain, cerebellum, and the hippocampal formation (Coy et al. 2002). Although, the biological function of

mammalian NAV3 protein remains unknown, a *Caenorhabditis elegans* gene named unc-53, highly homologous to NAV3, plays a pivotal role in axon guidance. All of these results suggest that a molecular defect of DAP12 on human monocytes deregulates the gene network pivotal for maintenance of myeloid cell function involved in bone homeostasis, immune function, and neuronal function in NHD.

References

Bianchin MM, Capella HM, Chaves DL, Steindel M, Grisard EC, Ganev GG, da Silva Júnior JP, Neto Evaldo S, Poffo MA, Walz R, Carlotti Júnior CG, Sakamoto AC (2004) Nasu-Hakola disease (polycystic lipomembranous osteodysplasia with sclerosing leukoencephalopathy—PLOSL): a dementia associated with bone cystic lesions. From clinical to genetic and molecular aspects. Cell Mol Neurobiol 24:1–24

Bijli KM, Fazal F, Minhajuddin M, Rahman A (2008) Activation of Syk by protein kinase C-δ regulates thrombin-induced intercellular adhesion molecule-1 expression in endothelial cells via tyrosine phosphorylation of RelA/p65. J Biol Chem 283:14674–14684

Coy JF, Wiemann S, Bechmann I, Bächner D, Nitsch R, Kretz O, Christiansen H, Poustka A (2002) Pore membrane and/or filament interacting like protein 1 (POMFIL1) is predominantly expressed in the nervous system and encodes different protein isoforms. Gene 290:73–94

Divanovic S, Trompette A, Petiniot LK, Allen JL, Flick LM, Belkaid Y, Madan R, Haky JJ, Karp CL (2007) Regulation of TLR4 signaling and the host interface with pathogens and danger: the role of RP105. J Leukoc Biol 82:265–271

Kaifu T, Nakahara J, Inui M, Mishima K, Momiyama T, Kaji M, Sugahara A, Koito H, Ujike-Asai A, Nakamura A, Kanazawa K, Tan-Takeuchi K, Iwasaki K, Yokoyama WM, Kudo A, Fujiwara M, Asou H, Takai T (2003) Osteopetrosis and thalamic hypomyelinosis with synaptic degeneration in DAP12-deficient mice. J Clin Invest 111:323–332

Klünemann HH, Ridha BH, Magy L, Wherrett JR, Hemelsoet DM, Keen RW, De Bleecker JL, Rossor MN, Marienhagen J, Klein HE, Peltonen L, Paloneva J (2005) The genetic causes of basal ganglia calcification, dementia, and bone cysts: DAP12 and TREM2. Neurology 64:1502–1507

Mócsai A, Ruland J, Tybulewicz VL (2010) The SYK tyrosine kinase: a crucial player in diverse biological functions. Nat Rev Immunol 10:387–402

Nataf S, Anginot A, Vuaillat C, Malaval L, Fodil N, Chereul E, Langlois JB, Dumontel C, Cavillon G, Confavreux C, Mazzorana M, Vico L, Belin MF, Vivier E, Tomasello E, Jurdic P (2005) Brain and bone damage in KARAP/DAP12 loss-of-function mice correlate with alterations in microglia and osteoclast lineages. Am J Pathol 166:275–286

Numasawa Y, Yamaura C, Ishihara S, Shintani S, Yamazaki M, Tabunoki H, Satoh JI (2011) Nasu-Hakola disease with a splicing mutation of TREM2 in a Japanese family. Eur J Neurol 18:1179–1183

Otero K, Turnbull IR, Poliani PL, Vermi W, Cerutti E, Aoshi T, Tassi I, Takai T, Stanley SL, Miller M, Shaw AS, Colonna M (2009) Macrophage colony-stimulating factor induces the proliferation and survival of macrophages via a pathway involving DAP12 and β-catenin. Nat Immunol 10:734–743

Roumier A, Béchade C, Poncer JC, Smalla KH, Tomasello E, Vivier E, Gundelfinger ED, Triller A, Bessis A (2004) Impaired synaptic function in the microglial KARAP/DAP12-deficient mouse. J Neurosci 24:11421–11428

Satoh JI, Tabunoki H, Ishida T, Yagishita S, Jinnai K, Futamura N, Kobayashi M, Toyoshima I, Yoshioka T, Enomoto K, Arai N, Arima K (2011) Immunohistochemical characterization of microglia in Nasu-Hakola disease brains. Neuropathology 31:363–375

Stefano L, Racchetti G, Bianco F, Passini N, Gupta RS, Panina Bordignon P, Meldolesi J (2009) The surface-exposed chaperone, Hsp60, is an agonist of the microglial TREM2 receptor. J Neurochem 110:284–294

Tanaka J (2000) Nasu-Hakola disease: a review of its leukoencephalopathic and membranolipodystrophic features. Neuropathology 20:S25–S29

Turnbull IR, Colonna M (2007) Activating and inhibitory functions of DAP12. Nat Rev Immunol 7:155–161

Turnbull IR, Gilfillan S, Cella M, Aoshi T, Miller M, Piccio L, Hernandez M, Colonna M (2006) Cutting edge: TREM-2 attenuates macrophage activation. J Immunol 177:3520–3524

Uz E, Alanay Y, Aktas D, Vargel I, Gucer S, Tuncbilek G, von Eggeling F, Yilmaz E, Deren O, Posorski N, Ozdag H, Liehr T, Balci S, Alikasifoglu M, Wollnik B, Akarsu NA (2010) Disruption of ALX1 causes extreme microphthalmia and severe facial clefting: expanding the spectrum of autosomal-recessive ALX-related frontonasal dysplasia. Am J Hum Genet 86: 789–796